THE JOURNAL OF BIOLOGICAL CHEMISTRY VOL. 287, NO. 53, pp. 44345–44360, December 28, 2012

Canonical Transient Receptor Potential Channel 2 (TRPC2) as a Major Regulator of Calcium Homeostasis in Rat Thyroid FRTL-5 Cells

IMPORTANCE OF PROTEIN KINASE C δ (PKCδ) AND STROMAL INTERACTION MOLECULE 2 (STIM2)[*] [S]

Received for publication, November 7, 2012 Published, JBC Papers in Press, November 9, 2012, DOI 10.1074/jbc.M112.374348

Pramod Sukumaran[‡], Christoffer Löf[‡§], Kati Kemppainen[‡], Pasi Kankaanpää[¶], Ilari Pulli[‡], Johnny Näsman[‡], Tero Viitanen[‖], and Kid Törnquist[‡**1]**

*From the [‡]Department of Biosciences, Åbo Akademi University, Tykistökatu 6A, 20520 Turku, Finland, [§]Turku Doctoral Programme of Biomedical Sciences, Kiinamyllynkatu 13, 20520 Turku, Finland, [¶]Department of Biochemistry and Food Chemistry, University of Turku, FI-20014 Turku, Finland, [‖]Institute of Biomedicine/Physiology, University of Helsinki, P. O. Box 63, 00014 Helsinki, Finland, and **Minerva Foundation Institute for Medical Research, Biomedicum Helsinki, 00270 Helsinki, Finland*

Background: The identity of calcium channels in thyroid is not defined.
Results: TRPC2 functions as a major regulator of calcium homeostasis in rat thyroid cells. TRPC2 appears to be receptor-regulated and participates in regulating ER calcium content.
Conclusion: We have defined a novel physiological role for TRPC2 channels.
Significance: TRPC2, by regulating STIM2, PKC expression, and SERCA activity, regulates calcium homeostasis in thyroid cells.

Mammalian non-selective transient receptor potential cation channels (TRPCs) are important in the regulation of cellular calcium homeostasis. In thyroid cells, including rat thyroid FRTL-5 cells, calcium regulates a multitude of processes. RT-PCR screening of FRTL-5 cells revealed the presence of TRPC2 channels only. Knockdown of TRPC2 using shRNA (shTRPC2) resulted in decreased ATP-evoked calcium peak amplitude and inward current. In calcium-free buffer, there was no difference in the ATP-evoked calcium peak amplitude between control cells and shTRPC2 cells. Store-operated calcium entry was indistinguishable between the two cell lines. Basal calcium entry was enhanced in shTRPC2 cells, whereas the level of PKCβ1 and PKCδ, the activity of sarco/endoplasmic reticulum Ca^{2+}-ATPase, and the calcium content in the endoplasmic reticulum were decreased. Stromal interaction molecule (STIM) 2, but not STIM1, was arranged in puncta in resting shTRPC2 cells but not in control cells. Phosphorylation site Orai1 S27A/S30A mutant and non-functional Orai1 R91W attenuated basal calcium entry in shTRPC2 cells. Knockdown of PKCδ with siRNA increased STIM2 punctum formation and enhanced basal calcium entry but decreased sarco/endoplasmic reticulum Ca^{2+}-ATPase activity in wild-type cells. Transfection of a truncated, non-conducting mutant of TRPC2 evoked similar results. Thus, TRPC2 functions as a major regulator of calcium homeostasis in rat thyroid cells.

In most if not all cells, calcium is the key regulator of a large number of cellular processes such as proliferation, motility, gene transcription, and apoptosis (1). To make such a broad spectrum of different actions possible, the cells have evolved multiple different mechanisms that regulate cellular calcium levels. Calcium can be mobilized from intracellular compartments by the activation of ryanodine receptors and inositol 1,4,5-trisphosphate (IP_3)[2] receptors. Calcium may enter the cells through several different types of calcium channels (both voltage-independent and -dependent channels), and Ca^{2+} ATPases in both the plasma membrane and intracellular membranes regulate the transport of calcium out of the cell or into intracellular compartments.

In thyroid cells, including rat thyroid FRTL-5 cells, several investigations have shown that changes in intracellular calcium regulate a multitude of central processes. These include the regulation of iodide efflux (2–4) and the regulation of both proliferation and synthesis of DNA (5, 6). Furthermore, the TSH-evoked effects in thyroid cells may also be modified by changes in intracellular calcium (2, 7). In addition, the regulation of TSH receptor expression (8) as well as the expression and dimerization of thyroglobulin (9, 10) is dependent on changes in intracellular calcium. Many agonists (*e.g.* ATP, ADP, UTP, and sphingosine 1-phosphate) and TSH evoke potent changes in intracellular free calcium through activation of G-protein-coupled receptors (11–16). Part of these changes in intracellular free calcium occurs through IP_3-evoked release of calcium sequestered in the endoplasmic reticulum. The release

* This work was supported by the Academy of Finland, the Sigrid Juselius Foundation, the Centre of Excellence in Cell Stress and Molecular Ageing (Åbo Akademi University), the Magnus Ehrnrooth Foundation, and the Receptor Research Program (Åbo Akademi University and University of Turku).
[S] This article contains supplemental Figs. 1–4 and Tables 1 and 2.
[1] To whom correspondence should be addressed: Dept. of Biosciences, Åbo Akademi University, Biocity, Tykistökatu 6A, 20520 Turku, Finland. Tel.: 35822154748; Fax: 35822154748; E-mail: ktornqvi@abo.fi.

[2] The abbreviations used are: IP_3, inositol 1,4,5-trisphosphate; TRPC, transient receptor potential canonical cation channel; STIM, stromal interaction molecule; SERCA, sarco/endoplasmic reticulum Ca^{2+}-ATPase; ER, endoplasmic reticulum; TSH, thyrotropin; SOCE, store-operated calcium entry; Tg, thapsigargin; DAG, diacylglycerol; OAG, *1-oleoyl-2-acetyl-sn-glycerol*.

of sequestered calcium then results in a profound entry of extracellular calcium into the cytosol due to store-operated calcium entry (SOCE) (17). Furthermore, receptor-operated calcium entry pathways are also present as the FRTL-5 cells express several P2X ionotropic receptors (6).

In the present study, we showed that FRTL-5 cells express only the TRPC2 channel of the TRPC family of calcium channels. This channel has been shown previously to be of importance only in ZP3-evoked calcium entry into sperm in rodents (18), pheromone-evoked signaling in the vomeronasal organ (19, 20), and regulation of erythropoietin-evoked calcium influx in erythroid cells (21). TRPC2 mediates both receptor-operated calcium entry and SOCE (18, 21). As TRPC2 seems to be of great importance in regulating the function of FRTL-5 cells (22), we investigated the effect of TRPC2 on calcium homeostasis in FRTL-5 cells. We show that the ATP-evoked entry of calcium is mediated, at least in part, by TRPC2. Furthermore, TRPC2, via protein kinase C (PKC) and STIM2, seems to have a role in regulating basal calcium levels and ER calcium content in thyroid cells. Thus, we have defined a novel physiological role for the TRPC2 channel.

EXPERIMENTAL PROCEDURES

Culture medium, serum, and hormones except bovine TSH were purchased from Invitrogen and Sigma-Aldrich. Bovine TSH was obtained from Dr. A. F. Parlow and the National Hormone and Pituitary Program (National Institutes of Health, Bethesda, MD). Culture dishes were obtained from Falcon Plastics (Oxnard, CA). Fura-2/AM, penicillin/streptomycin, and trypsin were from Invitrogen, and thapsigargin was from Enzo Life Sciences (Farmingdale, NY). mCherry-STIM1, YFP-STIM2, and TRPC2 plasmids were a kind gift from Dr. Richard S. Lewis (Stanford University), Dr. Tobias Meyer (Stanford University), and Dr. Catherine Dulac (Harvard University), respectively. Orai1 R91W plasmid and Orai1 S27A/S30A plasmid were from Dr. Anjana Rao (Harvard University) and Dr. Stefan Feske (New York University), respectively. The truncated form of TRPC2 (TRPC2-DN) was obtained from Dr. Genevieve Bart (University of Eastern Finland) (23). TRPC2DN is C-terminally truncated after the fifth transmembrane segment, lacks the pore region of the channel, and has a dominant negative effect (23). PKCα, -βI, -βII, -δ, -γ, -ζ, -η, and -ϵ antibodies were from Santa Cruz Biotechnology (Santa Cruz, CA). TRPC2 antibody was obtained from Novus Biologicals (Littleton, CO). The secondary antibodies used were horseradish peroxidase-conjugated anti-mouse and anti-rabbit antibodies from Sigma-Aldrich. PKC classical (CSVEIWD) and PKCδ (MRAAEDPM) activator peptides coupled to a membrane-permeable peptide (CYGRKKRRQRRR) (24, 25) were from KAI Pharmaceuticals (South San Francisco, CA).

Cell Culture—Rat thyroid FRTL-5 cells were grown in Coon's modified Ham's F-12 medium supplemented with 5% calf serum and six hormones (10 μg/ml insulin, 5 μg/ml transferrin, 10 nM hydrocortisone, 10 ng/ml tripeptide Gly-L-His-L-Lys, 0.3 milliunit/ml TSH, and 10 ng/ml somatostatin) in a water-saturated atmosphere of 5% CO_2 and 95% air at 37 °C. The medium for the TRPC knockdown cells and their controls contained puromycin (1 μg/ml). The cells were grown for 7–8 days, incorporating two to three changes of medium with the final medium change 24 h before an experiment.

Generation of Stable TRPC2 Knockdown Cell Lines—FRTL-5 cells were plated on 12-well plates. The following day, transfections were carried out with FuGENE HD (Roche Applied Science) and shRNA plasmids (SABiosciences, Frederick, MD) according to the manufacturers' instructions. 48 h post-transfection, untransfected cells were killed with 1 μg/ml puromycin. Puromycin was included in the growth medium from there on. The insert sequences used were GGAATCTCATTCGATGCATAC for the negative control and TCGCCCAACTGGACTGAGATTGT for TRPC2 (22).

Measurement of $[Ca^{2+}]_i$—Cells were grown in 35-mm cell culture dishes on polylysine-coated coverslips (diameter, 2.5 cm). After 2–4 days of culture, the cells were washed in HBSS buffer (118 mM NaCl, 4.6 mM KCl, 1 mM $CaCl_2$, 10 mM glucose, and 20 mM HEPES, pH 7.4) and incubated with Fura-2/AM (final concentration, 2 μM) for 30 min at 37 °C. After washing the cells once, the coverslip was mounted on an Axiovert 35 inverted microscope with a Fluor 40× objective. The excitation filters were set at 340 and 380 nm. Excitation light was obtained using an XBO 75W/2 xenon lamp. Emission was measured at 510 nm. The shutter was controlled by a Lambda 10-2 control device (Sutter Instruments, Novato, CA). Fluorescence images were collected with a SensiCam 12-bit charge-coupled device camera (PCO/CD Imaging, Kelheim, Germany). Images were taken every 3 s to avoid bleaching, and the images were processed using Axon Imaging Workbench (6.0) software (Axon Instruments, Foster City, CA). The results are given as the 340/380 nm ratio. All the experiments were performed at 37 °C. The data shown were calculated from the changes in $[Ca^{2+}]_i$ from all cells measured, *i.e.* both responding and non-responding cells. When experiments were performed in calcium-free buffer, the cells were perfused with calcium-free buffer (containing 0.1 mM EGTA) for 1 min, then the measurement was started, and after 1 min, the cells were stimulated. For experiments on permeabilized cells, cells were loaded with 3 μM Mag-Fura/AM for 45 min at 37 °C and then washed with KCl rinse buffer (125 mM KCl, 25 mM NaCl, 10 mM HEPES, and 0.2 mM $MgCl_2$, pH 7.25). Cells were then permeabilized with intracellular buffer (KCl rinse buffer with 200 μM $CaCl_2$ and 500 μM EGTA, pH 7.25) containing 10 μg/ml digitonin. When ~80% of the cells were permeabilized, excess digitonin was rinsed away by perfusion with intracellular buffer (26).

Electrophysiology—FRTL-5 cells were plated at low density onto 13-mm coverslips kept in 24-well plates and grown in Coon's 6H medium as above for 2–6 days before the experiments. Recordings were done at a room temperature of 23–25 °C in a recording chamber (volume, 200 μl) that was continuously perfused (flow rate, 700 μl/min).

The extracellular solution contained 150 mM NaCl, 5.4 mM CsCl, 3.0 mM $CaCl_2$, and 5 mM HEPES. The pH was adjusted to 7.4 with NaOH. Patch pipettes (3–8 megaohms) were filled with a solution containing 135 mM cesium methanesulfonate, 10 mM CsCl, 4.25 mM Na_2ATP, 0.5 mM LiGTP, 125 μM EGTA, 10 mM HEPES, pH 7.20 with CsOH.

Whole-cell membrane currents (27) were recorded with an EPC-9 amplifier and Pulse software (HEKA Elektronik, Lam-

brecht, Germany). Currents were allowed to stabilize for at least 5 min before the experiments were started. The voltage clamp protocol used had three segments (step-ramp-step): a 50-ms step to a holding voltage (V_h) of −90 mV was followed by an ascending ramp of 200 ms in duration (+0.5 mV ms^{-1}) after which the end voltage of 10 mV was maintained for 50 ms. The protocol was applied at 2-s intervals, and the cells were held at −10 mV between the stimulation. Whole-cell capacitance and series resistance were at least 80% compensated for, and membrane currents were sampled at 2 kHz and low pass-filtered off-line at 1 kHz.

The application of ATP (50 μM) was used to evoke membrane currents in the cells. Data analysis was done using PulseFit (HEKA Elektronik) and Origin (OriginLab, Northampton, MA) software. The first trace of each ATP experiment was subtracted as a leak after which the current minimum at the beginning of the ramp segment was detected. The liquid junction potentials were estimated with JPCalc software (28). A liquid junction potential of 15 mV was subtracted off-line to represent reversal potential (E_R) values. Statistical significance was tested with a non-paired *t* test.

Qualitative RT-PCR—FRTL-5 cells were grown on 60-mm plates. The plates were washed once with ice-cold PBS, and RNA was isolated using the Aurum total RNA minikit (Bio-Rad) according to the manufacturer's instructions. RNA quality and integrity were tested by absorbance spectrometry and by agarose gel electrophoresis. RNA concentrations were determined using the RiboGreen RNA quantitation reagent (Molecular Probes). Reverse transcriptase reactions were performed on 0.25 μg of RNA using SuperScript III reverse transcriptase (Applied Biosystems) and oligo$(dT)_{15}$ primers (Promega) following the manufacturers' instructions.

The TRPC primer sequences for RT-PCR were obtained from the literature and are listed in supplemental Table 1. The PCR was performed in 50-μl reactions (5 μl of cDNA; 1 μM primers; a 200 nM concentration each of dATP, dCTP, dGTP, and dCTP; 0.5 unit of DyNAzyme EXT DNA polymerase) on a Mastercycler gradient thermal cycler (Eppendorf, Hamburg, Germany) with the activation step at 94 °C for 5 min followed by 30 cycles with strand separation at 94 °C for 30 s and annealing for 60 s followed by elongation at 72 °C for 60 s. Negative controls in which reverse transcriptase was omitted from the cDNA reaction were performed to rule out that the RNA samples were not contaminated with genomic DNA. The PCR products was separated by gel electrophoresis and visualized with ethidium bromide under UV light. A quantitative PCR assay was performed to check the percentage of TRPC2 knockdown (22).

Primer sequences for TRPC2 variants, melting temperatures, and annealing temperatures are presented in supplemental Table 2. Melting temperatures were calculated with the modified nearest neighbor method as instructed by the DyNAzyme EXT data sheet. Gels were visualized and photographed with the AlphaImager HP system (ProteinSimple, Santa Clara, CA).

PCR product bands were extracted from the gel with the GeneJet gel extraction kit (Fermentas) according to the manufacturer's instructions, and DNA preparations were further purified by ethanol precipitation if necessary. Sequencing of PCR products was performed by the Turku Centre for Biotechnology (BTK) sequencing service. For each PCR product, one of its PCR primers was also used as a sequencing primer.

Western Blotting—The cells were washed three times with ice-cold PBS and lysed in cell lysis buffer (10 mM Tris, pH 7.7, 150 mM NaCl, 7 mM EDTA, 0.5% Nonidet P-40, 0.2 mM phenylmethylsulfonyl fluoride (PMSF), and 0.5% g/ml leupeptin), the lysates were centrifuged at 13,000 rpm for 15 min at 4 °C, and the supernatants were collected. Protein concentration was determined using the BCA™ protein assay kit (Pierce). The samples were then stored at −20 °C. Samples were subjected to SDS-PAGE (10% polyacrylamide). The proteins were transferred onto nitrocellulose membrane (PerkinElmer Life Sciences) by wet blotting. Western blot analysis was performed using specific primary and secondary antibodies to the indicated proteins. The proteins were detected by enhanced chemiluminescence. Densitometric analysis was performed using ImageJ software, and results were corrected for protein loading by normalization for Hsc-70 expression. The normalized data are shown in the figure legends.

Transfection with Small Interfering RNA (siRNA) and Plasmid Constructs—FRTL-5 (4,000,000 cells) were transfected with 5 μM siRNA using electroporation with an exponential protocol with a voltage of 300 V and a capacitance of 975 microfarads. The transfected cells were plated on 35-mm dishes and used for calcium measurement after 48 h. All siRNA constructs were purchased from Ambion Inc. (Austin, TX). The TRPC2 cDNA was cut out from the pBluescript cloning vector with BamHI and NcoI. After blunting the NcoI site, the fragment was subcloned into pEGFP-C3 (Clontech) cut with BglII and SmaI. By using the BamHI site, the initiator methionine was deleted from the TRPC2 gene, and the fusion generated the EGFP-TRPC2 construct. The truncated form of TRPC2 is the N-terminal cytosolic domain with one transmembrane domain, modulating channel trafficking to the cell membrane or inhibiting the activation of native TRPC2 (29).

SERCA Activity Assay—For measuring the SERCA activity, the cells were grown on 35-mm plates, harvested, and lysed using lysis buffer (see above). The samples were centrifuged at 10,000 rpm for 15 min at 4 °C. The supernatant was discarded, and the sediment was dissolved in HBSS buffer and sonicated, and SERCA activity was measured according to the manufacturer's instructions (Nanjing Jiancheng Bioengineering Inst., Nanjing City, China) (30). The kit measures inorganic phosphorus (P_i) content produced from ATPase activity in the samples when ATP is broken down to ADP and P_i. 1 μmol of P_i produced by ATPase-catalyzed ATP decomposition/h/mg of cell protein is considered as 1 ATPase activity unit (μmol of P_i/mg of protein/h). The samples were analyzed at 590 nm using a Viktor fluorescence analyzer (PerkinElmer Life Sciences), and the colorimetric reading was normalized with the respective total protein concentrations.

Confocal Microscopy and Image Analysis—The cells were transfected as mentioned above with mCherry-STIM1 and YFP-STIM2. The cells were plated onto polylysine-coated coverslips. The cells were cultured for 48 h with a change of culture medium after 24 h. After stimulation with 0.1 mM EGTA for 10 min, the coverslips were washed three times with PBS, fixed

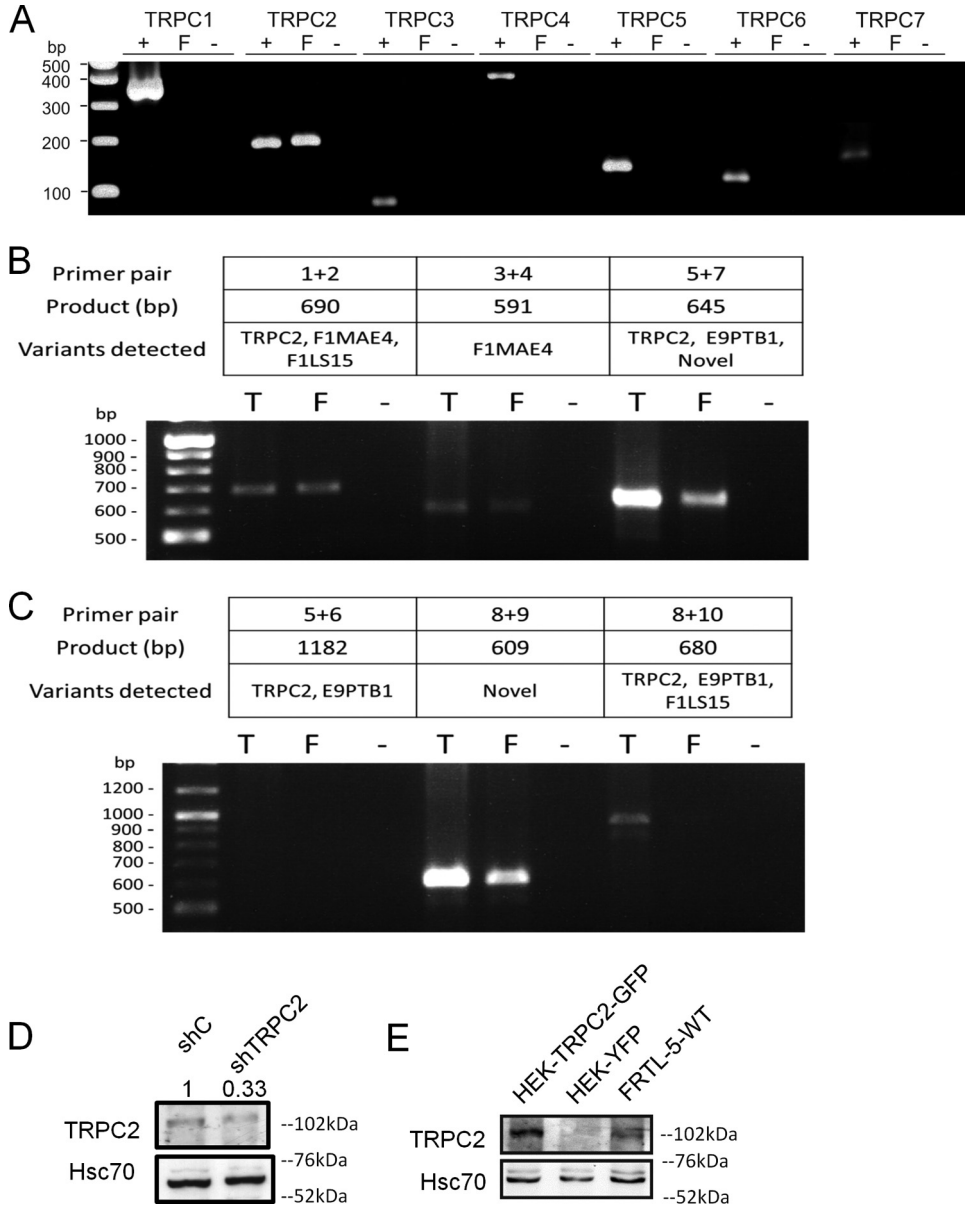

FIGURE 1. **Expression of the TRPC2 channel in FRTL-5 cells and knockdown of the channel using shRNA.** *A*, RT-PCR screen of TRPC isoforms in FRTL-5 cells. + denotes the positive control RNA used for the primers. Rat testis RNA was used for all TRPCs except TRPC3 for which RNA from PC-12 cells was used. FRTL-5 cell RNA is denoted by the *letter F*. − is a negative control with FRTL-5 cell RNA that has not been reverse transcribed. *B* and *C*, FRTL-5 cells express TRPC2 splice variants F1MAE4 and Novel but not the full-length protein. Primers were designed to discriminate between the different TRPC2 splice variants. For each primer pair, the expected product size, the variants detected by the primer pair, and the obtained PCR products are shown. The templates are rat testis cDNA (*T*), FRTL-5 cDNA (*F*), and FRTL-5 RNA (−). *D*, Western blots showing the expression of TRPC2 in shC and shTRPC2 cells (shC, 1.0 ± 0.20; shTRPC2 0.33 ± 0.07; $n = 3$; $p < 0.05$). The *number* above the blot indicates the relative amount of protein. *E*, Western blot of HEK-293 cells transfected with TRPC2 (*HEK-TRPC2-GFP*), mock-transfected HEK-293 cells (*HEK-YFP*), and wild-type FRTL-5 cells (*FRTL-5-WT*). The blot is representative of three experiments with similar results.

using 4% paraformaldehyde, and mounted on a slide with Mowiol. Fifteen confocal optical sections with optimized image acquisition settings (Nyquist resolution; pinhole, 1 airy unit; no saturation) were acquired of each sample. The cells imaged were randomly selected from those with sufficient YFP or mCherry expression but no extensive overexpression. All images were acquired with exactly the same settings and in one continuous session (to make sure that sample quality, age, and imaging conditions were the same for each sample). All images were taken of the cell membrane near the glass surface at the level where the membrane first comes properly into focus. Experiments were performed with AxioObserver Z1 (63×/1.4 oil immersion objective) equipped with LSM510 (Carl Zeiss Inc., Jena, Germany). Image analysis was carried out using BioImageXD software (31). Hybrid median filtering was first applied to remove noise, and then Otsu thresholding was used to automatically detect meaningful fluorescence signal. Isolated image areas only 1–2 voxels in size were removed as noise, and the average intensity of the remaining voxels was calculated. The hybrid median filtered images were then thresholded again with a fixed value that retained only the most prominent membrane patches.

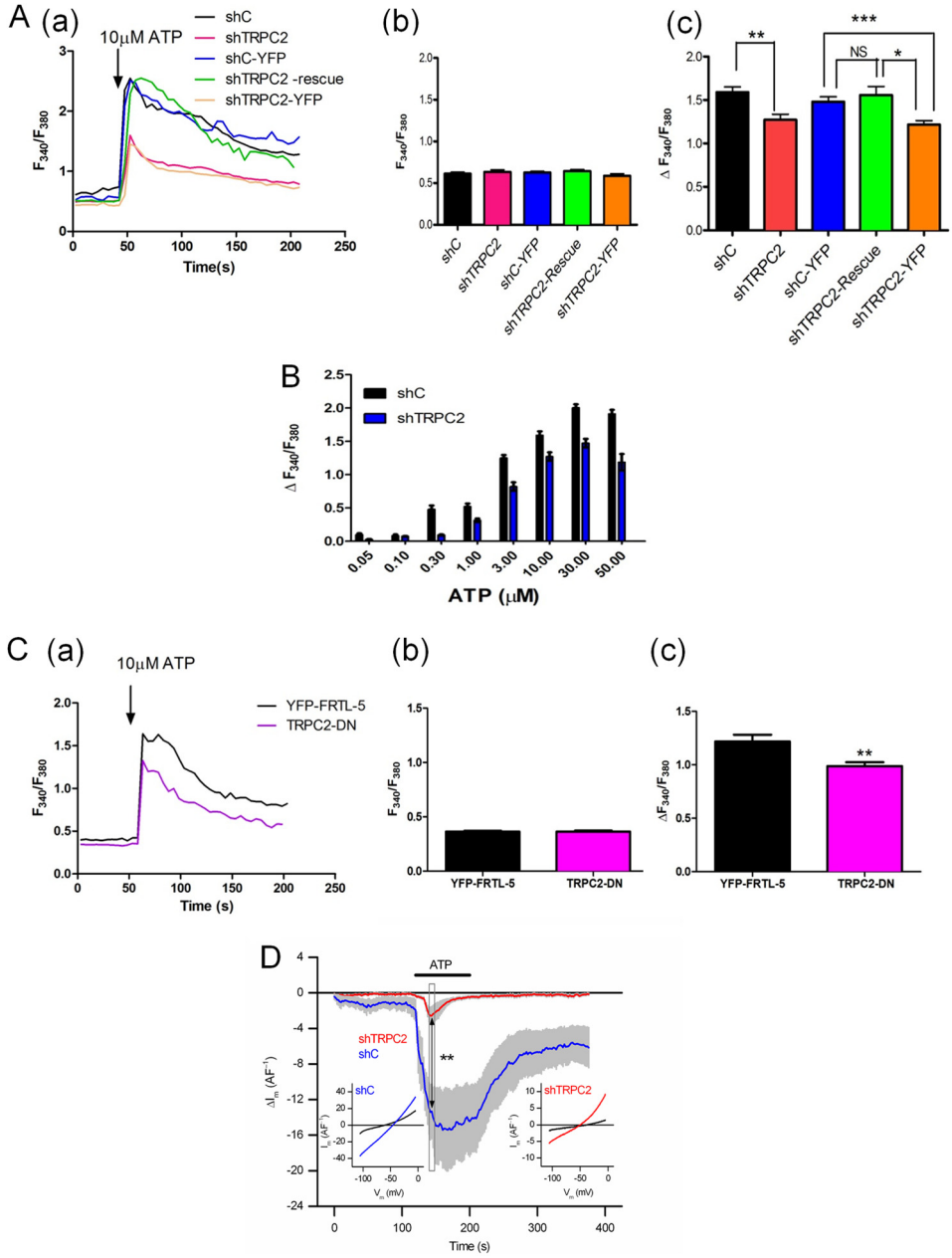

FIGURE 2. **ATP-evoked calcium entry is decreased in shTRPC2 cells.** *A*, *panel a*, representative traces of shC, shTRPC2, shC-YFP, shTRPC2-YFP, and shTRPC2-rescue cells stimulated with 10 μM ATP in a calcium-containing buffer. *Panel b*, bar diagram showing the basal Fura-2 ratio before stimulating with 10 μM ATP. *Panel c*, bar diagram showing the ATP-evoked calcium peak amplitude after adding 10 μM ATP. The *bars* give the mean ± S.E. (*error bars*) of at least 45 cells in each group (***, $p < 0.001$; **, $p < 0.01$; *, $p < 0.05$; *NS*, not significant). *B*, concentration-response curve for ATP-evoked calcium peak amplitude in $[Ca^{2+}]_i$ in a calcium-containing buffer in shC cells and shTRPC2 cells. The *bars* give the mean ± S.E. (*error bars*) of at least 60 cells in each group. A significant (***, $p < 0.001$) difference was observed between the shC cells and the shTRPC2 cells. *C*, *panel a*, representative traces of wild-type FRTL-5 cells transfected with YFP or a non-conducting mutant of TRPC2 (TRPC2-DN) and stimulated with 10 μM ATP in a calcium-containing buffer. *Panel b*, bar diagram showing the basal Fura-2 ratio before stimulating with 10 μM ATP. *Panel c*, bar diagram showing the calcium peak amplitude after adding 10 μM ATP. The *bars* give the mean ± S.E. (*error bars*) of at least 35 cells in each group (**, $p < 0.01$). All the data shown were calculated from the changes in $[Ca^{2+}]_i$ from all cells measured, *i.e.* both responding and non-responding cells. *D*, ATP (50 μM)-evoked membrane currents are suppressed in shTRPC2 cells (*red*; $n = 8$) compared with shC cells (*blue*; $n = 10$). The ATP responses of shTRPC2 cells appeared as brief transients that recovered quickly. The responses in shC cells were more sustained and showed only partial recovery. The time window used for statistical analysis is delineated with a *gray line*. In the *insets*, the current (*I*)-voltage (*V*) characteristics of membrane currents of shC cells (*left*) and shTRPC2 cells (*right*) are shown in the absence (*black*) and presence of ATP (*blue* and *red*) (**, $p < 0.01$). Perfusion with ATP evoked clear responses in seven of eight shC cells and six of 10 shTRPC2 cells. *F*, farad.

Object separation was then used to separate patches touching each other, and after removing objects 1–2 voxels in size, the number of patches was calculated. For every cell, the result was divided by the number of voxels analyzed in the first step (representing the amount of plasma membrane analyzed). This was done to compensate for variations in cell size. The final results were statistically analyzed with a two-tailed heteroscedastic *t* test.

Statistics—The results are expressed as the mean ± S.E. Statistical analysis was made using Student's *t* test. When three or

more means were tested, one-way analysis of variance and Bonferroni's post hoc test were used. A p value below 0.05 was considered statistically significant.

RESULTS

Expression of the TRPC2 Channel in FRTL-5 Cells—RT-PCR screening of TRPCs showed that only TRPC2 was expressed in FRTL-5 cells (Fig. 1*A*). There are five TRPC2 splice variants listed in the Ensembl Genome Browser database: full-length TRPC2, Novel, E9PTB1, F1LS15, and F1MAE4. We designed PCR primers to determine which of these variants are expressed in FRTL-5 cells. The areas of mRNA detected by each primer pair are presented in supplemental Fig. 1A.

Based on the PCR products (Fig. 1, *B* and *C*), FRTL-5 cells express only variants F1MAE4 and Novel. Primer pairs 5 + 6 and 8 + 10 did not give the expected products, indicating that full-length TRPC2, E9PTB1, and F1LS15 are not expressed.

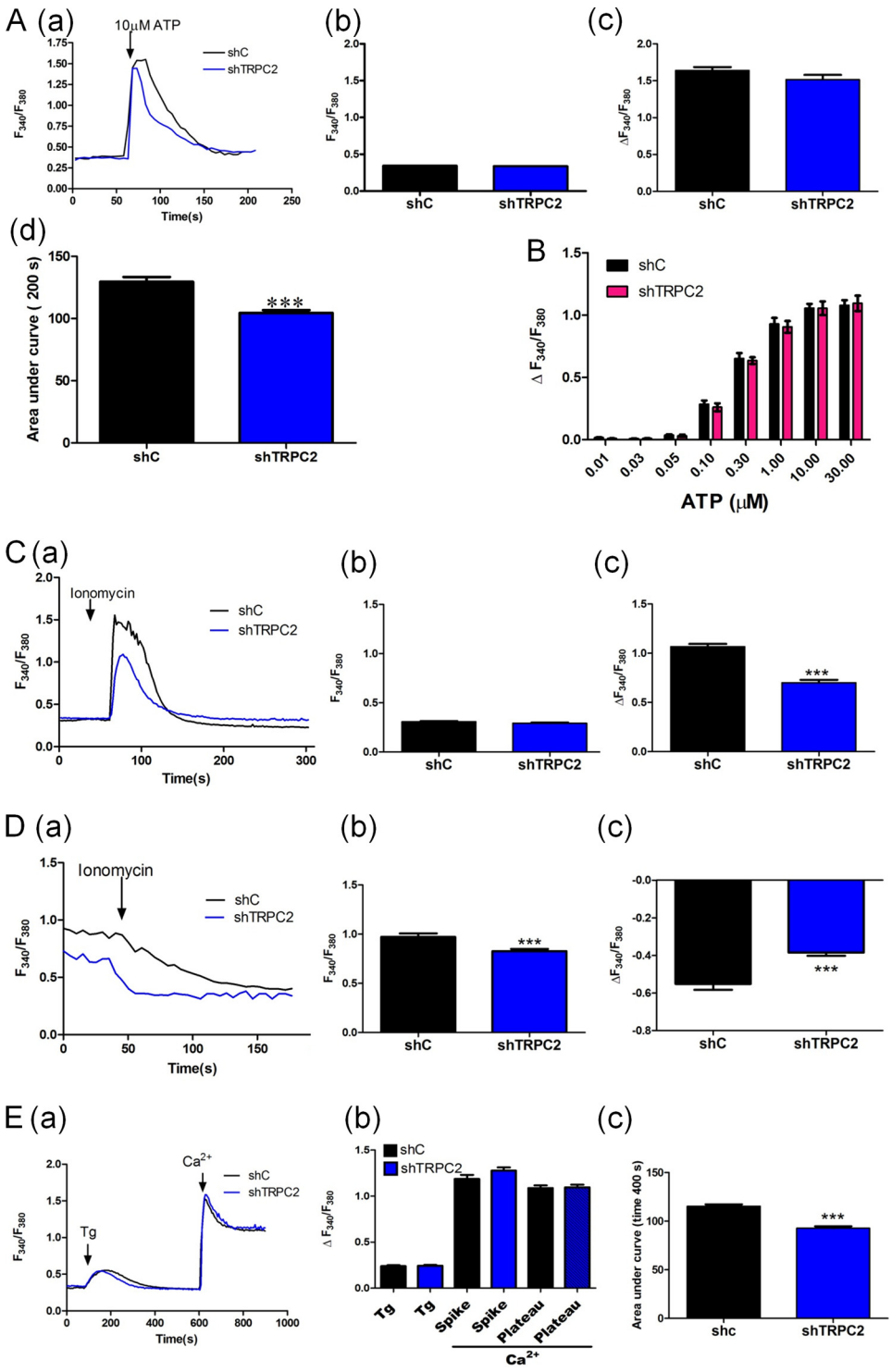

The bands of expected size given by primer pairs 1 + 2 and 3 + 4 and by primer pairs 5 + 7 and 8 + 9 can be explained by expression of F1MAE4 and Novel, respectively. Sequencing was used to confirm that the FRTL-5 PCR products were derived from TRPC2 variants.

We next made a stable TRPC2 knockdown cell line (shTRPC2) using the shRNA technique (22). As measured on the mRNA level with quantitative real time PCR, the knockdown was 90 (22) and 66% (shC, 1.0 ± 0.20; shTRPC2; 0.33 ± 0.07; $n = 3$; $p < 0.05$) on the protein level (Fig. 1*D*). To study the specificity of the antibody used, we transfected TRPC2 to HEK-293 cells (which do not endogenously express TRPC2). As can be seen in Fig. 1*E*, the antibody detected TRPC2 in TRPC2-transfected cells but not in mock-transfected control cells.

ATP-evoked Calcium Entry Is Decreased in TRPC2 Knockdown Cells—ATP is a well known agonist evoking calcium signaling in FRTL-5 cells (7, 13, 32), but it is unclear which channels are responsible for ATP-evoked calcium entry. TRPC2 channels are activated by ATP-evoked stimulation (18). When shC and shTRPC2 cells were stimulated with ATP in a calcium-containing buffer, there was a marked reduction in the ATP-evoked calcium peak amplitude (*i.e.* $\Delta F_{340}/F_{380}$) in shTRPC2 cells compared with shC cells (Fig. 2*A*). This reduction was evident at all concentrations of ATP used (Fig. 2*B*). Importantly, transient transfection of TRPC2 in shTRPC2 (shTRPC2-rescue) rescued the ATP-evoked calcium peak amplitude (Fig. 2*A*). Knockdown of TRPC2 did not affect basal calcium levels in FRTL-5 cells (Fig. 2*A*). Transfection of a truncated, non-conducting mutant of TRPC2 (TRPC2-DN) in wild-type FRTL-5 cells also attenuated the ATP-evoked calcium peak amplitude (Fig. 2*C*). Patch clamp experiments also revealed a pronounced reduction in the ATP-evoked inward current in shTRPC2 cells compared with shC cells (Fig. 2*D*). The inward calcium peak amplitude of the ATP-evoked currents at −90 mV was significantly smaller in shTRPC2 cells (−2.4 ± 0.4 A farad^{-1}; $n = 10$) compared with shC cells (−13.6 ± 1.4 A farad^{-1}; $n = 8$; $p < 0.001$). Thus, a decreased expression of TRPC2 in FRTL-5 cells potently hampered ATP-evoked calcium entry.

Knockdown of TRPC2 Affects the ER Calcium Content but Not Store-operated Calcium Entry in shTRPC2 Cells—In a calcium-free buffer, we did not observe any differences in the ATP-evoked calcium peak amplitude between shTRPC2 cells and shC cells (Fig. 3*A*). There was no difference in any given concentration of ATP (Fig. 3*B*). However, a careful analysis of the ATP-evoked calcium peak amplitude in a calcium-free buffer showed that the areas under the ATP curve (*i.e.* calcium released from the ER) were slightly, but significantly, smaller in shTRPC2 cells compared with shC cells (Fig. 3*A*, *panel d*). This suggested that the calcium content in the ER was smaller in shTRPC2 cells compared with shC cells. To investigate this possibility further, we stimulated cells in a calcium-free buffer with 2 μM ionomycin, a potent, highly selective calcium ionophore (33). As can be seen in Fig. 3*C*, the release of calcium from the ER in shTRPC2 cells was significantly smaller compared with the release seen in shC cells. In addition, in permeabilized cells in which the ER was loaded with Mag-Fura, the ER calcium level as well as the amount of calcium released by ionomycin was significantly smaller in shTRPC2 cells compared with shC cells (Fig. 3*D*).

Thapsigargin (Tg) is a potent endoplasmic reticulum Ca^{2+}-ATPase inhibitor, depleting intracellular calcium stores and evoking substantial SOCE in FRTL-5 cells (17). Knockdown of TRPC2 channels did not attenuate the calcium peak amplitude evoked by 1 μM Tg (Fig. 3*E*). In shTRPC2 cells, the effect of readdition of calcium to cells treated with Tg in a calcium-free buffer did not in any way differ from that seen in shC cells, suggesting that TRPC2 mainly functions as a receptor-operated calcium channel in FRTL-5 cells (Fig. 3*E*). However, when the area under the curve for the Tg-evoked calcium response was measured, we observed that the response was significantly smaller in shTRPC2 cells compared with shC cells (Fig. 2*E*, *panel c*). Taken together, our results show that the calcium content in the ER was smaller in shTRPC2 cells compared with shC cells.

Knockdown of TRPC2 Increased Basal Calcium Entry and Decreased SERCA Activity in shTRPC2 Cells—In unstimulated shTRPC2 cells, we observed that readdition of calcium (final concentration, 1 mM) to these cells in a calcium-free buffer evoked an enhanced increase in $[Ca^{2+}]_i$ compared with shC cells (Fig. 4*A*). To further confirm our observation, the experiment was carried out by removing and readding calcium and measuring the increase in $[Ca^{2+}]_i$ in shC and shTRPC2 cells. Also in this experimental design, the increase in $[Ca^{2+}]_i$ was enhanced in shTRPC2 cells compared with shC cells (supplemental Fig. 1C). The difference in the increase in $[Ca^{2+}]_i$ was attenuated in rescue experiments where TRPC2 was transfected to shTRPC2 cells (Fig. 4*B*) and was mimicked by trans-

FIGURE 3. **Effect of knockdown of TRPC2 on ER calcium content and store-operated calcium entry.** *A*, *panel a*, representative trace of shC and shTRPC2 cells stimulated with 10 μM ATP in a calcium-free buffer. The cells were incubated in calcium-free buffer for 2 min before stimulating with ATP. *Panel b*, bar diagram showing the basal Fura-2 ratio before stimulating with 10 μM ATP. *Panel c*, bar diagram showing the ATP-evoked calcium peak amplitude after adding 10 μM ATP. *Panel d*, bar diagram showing the area under the ATP-evoked calcium peak amplitude (time, 0–200 s) for experiments shown in *panel a* (129.6 ± 3.88 and 104.6 ± 2.2 arbitrary units in shC and shTRPC2, respectively; ***, $p < 0.0001$). The *bars* give the mean ± S.E. (*error bars*) of at least 45 cells in each group. *B*, concentration-response curve for ATP-evoked calcium peak amplitude in a calcium-free buffer in shC cells and shTRPC2 cells. The *bars* give the mean ± S.E. (*error bars*) of at least 60 cells in each group. No significant difference was observed in any concentration. *C*, *panel a*, representative traces of shC and shTRPC2 cells stimulated with 2 μM ionomycin in a calcium-free buffer. *Panel b*, bar diagram showing the basal Fura-2 ratio before adding 2 μM ionomycin. *Panel c*, bar diagram showing the calcium peak amplitude after adding ionomycin. Each *bar* gives the mean ± S.E. (*error bar*) of at least 55 cells in each group (***, $p < 0.001$). *D*, *panel a*, effect of 2 μM ionomycin on ER calcium content in permeabilized shC and shTRPC2 cells loaded with Mag-Fura. The traces shown are mean traces of all measurements. *Panel b*, bar diagram showing the basal ER Fura-2 ratio before adding ionomycin. *Panel c*, bar diagram showing the decrease in ER calcium content after adding 2 μM ionomycin. Each *bar* gives the mean ± S.E. (*error bar*) of at least 60 cells in each group (***, $p < 0.001$). *E*, *panel a*, representative traces showing Tg (final concentration, 1 μM)-evoked changes in shC and shTRPC2 cells in calcium-free buffer and the effect of readdition of calcium (final concentration, 1 mM). *Panel b*, bar diagram showing the summary of experiments in *a*. Each *bar* gives the mean ± S.E. (*error bar*) of at least 110 cells in each group. *Panel c*, bar diagram showing the area under the Tg curve (time, 0–400 s) for experiments shown in *A* (115.4 ± 1.89 and 92.8 ± 2.03 arbitrary units in shC and shTRPC2, respectively; $p < 0.0001$). All the data shown were calculated from the changes in $[Ca^{2+}]_i$ from all cells measured, *i.e.* both responding and non-responding cells.

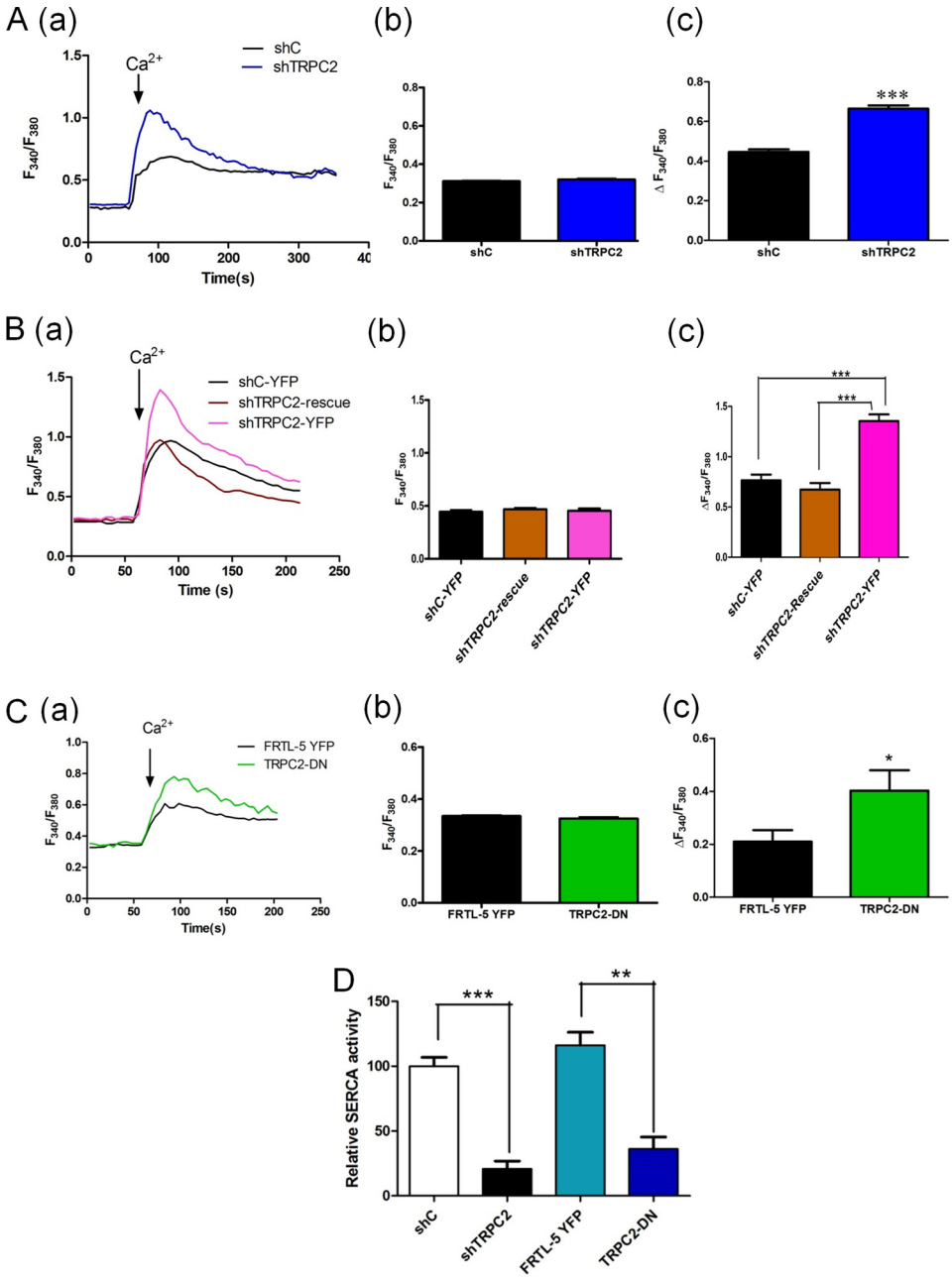

FIGURE 4. **Effect of knockdown of TRPC2 on basal calcium entry and SERCA activity.** *A*, *panel a*, representative traces of shC and shTRPC2 cells stimulated with 1 mM Ca^{2+} in a calcium-free buffer. *Panel b*, bar diagram showing the basal Fura-2 ratio before adding 1 mM Ca^{2+}. *Panel c*, bar diagram showing the increase in $[Ca^{2+}]_i$ after adding 1 mM Ca^{2+}. Each *bar* gives the mean ± S.E. (*error bar*) of at least 65 cells in each group (***, $p < 0.001$). *B*, *panel a*, re-expression of TRPC2 in shTRPC2 cells (shTRPC2-rescue) abolishes the difference in basal calcium entry between shTRPC2 and shC cells. *Panel b*, bar diagram showing the basal Fura-2 ratio before adding 1 mM Ca^{2+}. *Panel c*, bar diagram showing the increase in $[Ca^{2+}]_i$ after adding 1 mM Ca^{2+}. Each *bar* gives the mean ± S.E. (*error bar*) of at least 39 cells in each group (***, $p < 0.001$). *C*, *panel a*, representative traces showing addition of calcium (final concentration, 1 mM) to wild-type FRTL-5 cells transfected with YFP or a non-conducting mutant of TRPC2 (TRPC2-DN) in a calcium-free buffer. *Panel b*, bar diagram showing the basal Fura-2 ratio before adding 1 mM Ca^{2+}. *Panel c*, bar diagram showing the increase in $[Ca^{2+}]_i$ after adding 1 mM Ca^{2+}. The *bars* give the mean ± S.E. (*error bars*) of at least 48 cells in each group (*, $p < 0.05$). All the data shown were calculated from the changes in $[Ca^{2+}]_i$ from all cells measured, *i.e.* both responding and non-responding cells. *D*, comparison of SERCA activity in shC and shTRPC2 cells and wild-type FRTL-5 cells transfected with YFP or TRPC2-DN. Each *bar* gives the mean ± S.E. (*error bar*) of four separate measurements (**, $p < 0.01$; ***, $p < 0.001$).

fecting wild-type FRTL-5 cell with the non-conducting TRPC2-DN mutant (Fig. 4*C*). The decreased content of calcium in the ER (see Fig. 2, *A–E*) could be due to decreased SERCA activity (34, 35); thus, SERCA activity was measured (30). The results showed a decreased activity of SERCA in shTRPC2 cells compared with shC cells (Fig. 4*D*). In TRPC2-DN cells, the activity was also significantly decreased compared with control FRTL-5-YFP cells (Fig. 4*D*). Thus, the decreased ER calcium content and concomitant enhanced basal calcium entry in shTRPC2 cells were probably due to decreased SERCA activity.

Pretreatment with PKC Inhibitor GF109203X Increased Basal Calcium Influx and OAG-induced Increase in shC Cells—PKC is a potent regulator/inhibitor of calcium entry in FRTL-5 cells (17) and may also regulate calcium entry and the calcium

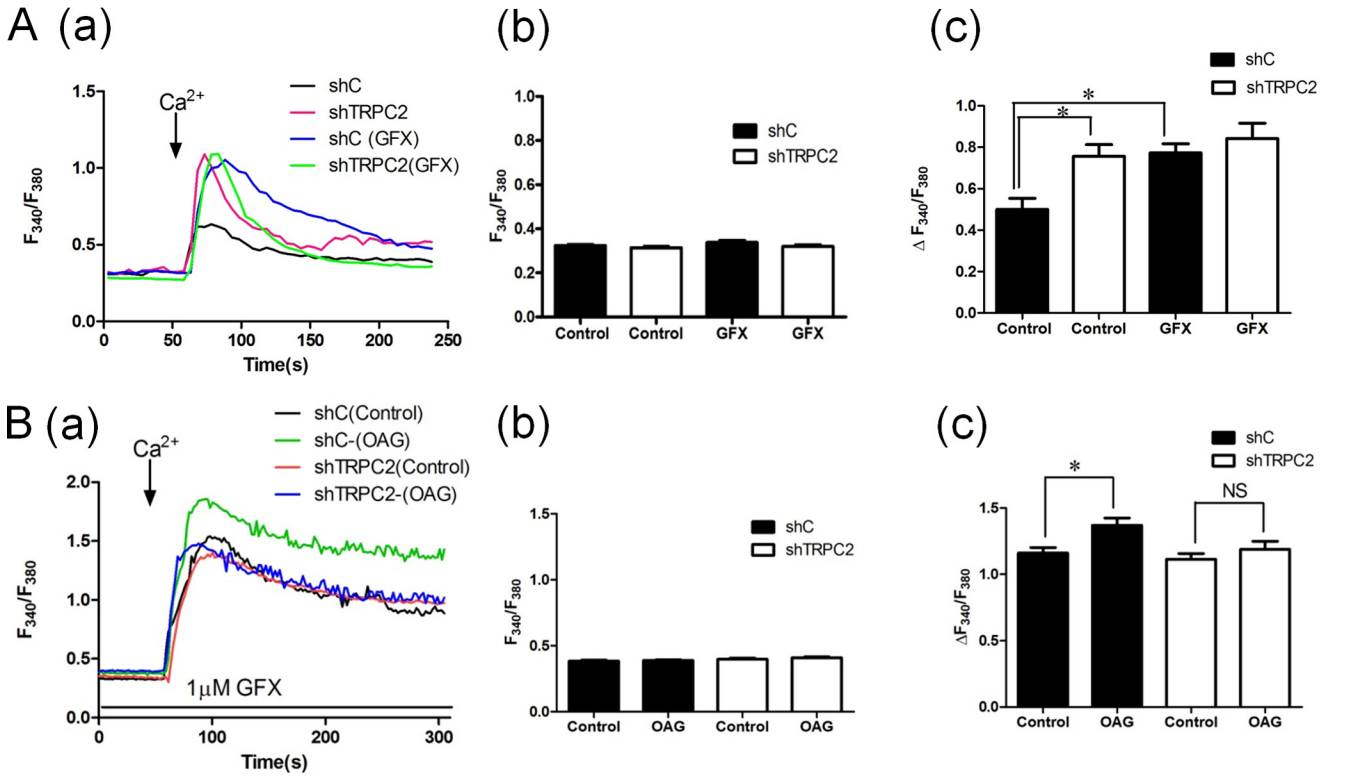

FIGURE 5. **Importance of PKC in regulating basal calcium entry in shC and shTRPC2 cells.** *A*, *panel a*, representative traces showing that pretreatment with GF109203X (*GFX*; 1 μM for 2 min) enhances calcium entry in shC cells to the same level as in shTRPC2 cells. *Panel b*, bar diagram showing the basal Fura-2 ratio before adding 1 mM Ca^{2+}. *Panel c*, bar diagram showing the increase in $[Ca^{2+}]_i$ after adding 1 mM Ca^{2+}. Each *bar* gives the mean ± S.E. (*error bar*) of at least 65 cells in each group (*, $p < 0.05$). *B*, *panel a*, representative traces showing that pretreatment with GF109203X (1 μM for 2 min) enhances 50 μM OAG-induced calcium entry in shC cells but not in shTRPC2 cells. *Panel b*, bar diagram showing the basal Fura-2 ratio before adding 1 mM Ca^{2+}. *Panel c*, bar diagram showing the increase in $[Ca^{2+}]_i$ after adding 1 mM Ca^{2+}. Each *bar* gives the mean ± S.E. (*error bar*) of at least 70 cells in each group (*, $p < 0.05$). All the data shown were calculated from the changes in $[Ca^{2+}]_i$ from all cells measured, *i.e.* both responding and non-responding cells.

content in the ER of several cell types. To test a possible role of PKC, we treated the cells with the PKC inhibitor GF109203X (1 μM for 2 min). GF109203X did not affect the increase in $[Ca^{2+}]_i$ when calcium was readded to shTRPC2 cells in a calcium-free buffer, but the increase in $[Ca^{2+}]_i$ in shC cells was enhanced to the same levels as in shTRPC2 cells (Fig. 5*A*). To check whether a receptor-operated channel is involved in FRTL-5 cells, the calcium peak amplitude increase was measured in cells pretreated with 1 μM GF109203X and 50 μM OAG (an analog of DAG) (supplemental Fig. 1C). The response was also studied in the wild-type FRTL-5 cells in which the addition of 100 μM OAG (in the presence of 1 μM GF109203X) evoked a rapid and substantial increase in $[Ca^{2+}]_i$ (supplemental Fig. 1D). Furthermore, 50 μM OAG enhanced the peak amplitude in basal calcium influx in the presence of 1 μM GF109203X in shC cells but not in shTRPC2 cells (Fig. 5*B*). These results point to a role of PKC in calcium regulation and are further proof of the existence of TRPC2 channels in FRTL-5 cells.

Decreased Expression of PKCβI and PKCδ in shTRPC2 Cells—Previous studies (36) have revealed the expression of PKC isoforms α, βI, βII, γ, η, ϵ, ζ, and δ in FRTL-5 cells. In shTRPC2 cells, the expression of PKCβI and PKCδ was decreased compared with control cells (Fig. 6*A* and supplemental Fig. 4, A and B). Pretreatment of wild-type FRTL-5 cells with a 5 μM concentration of a PKCδ activator (MRAAEDPM-CYGRKKRRQRRR) for 2 h attenuated the increase in $[Ca^{2+}]_i$ evoked by readdition of calcium in a calcium-free buffer (Fig. 6*B*). A PKCα and -β (classical; CSVEIWD-CYGRKKRRQRRR) activator did not reduce the increase in $[Ca^{2+}]_i$ (Fig. 6*C*), but the area under the curve for the calcium response was slightly, but significantly, smaller in magnitude compared with control cells (107 ± 3.7 and 95 ± 3.2 arbitrary units in control and PKC classical activator-treated cells, respectively; $p < 0.01$). PKCβ1 and PKCδ were also down-regulated in TRPC2-DN cells when compared with FRTL-5-YFP cells (Fig. 6, *D* and *E*). Hence, TRPC2 appears to regulate PKCδ and PKCβ1 expression, and PKCδ in turn seems to have a role in regulating basal calcium entry in FRTL-5 cells.

The STIM2 Protein Is Constitutively Translocated into Puncta in TRPC2 Knockdown Cells—It has been shown that the STIM proteins may regulate both basal calcium entry and calcium entry after calcium depletion of the ER (37). Thus, we overexpressed mCherry-tagged STIM1 or YFP-tagged STIM2 in our cells. Image analysis using the BioImageXD software (31) indicated that in unstimulated cells STIM2 showed an enhanced punctum formation in shTRPC cells compared with shC cells (Fig. 7, *A–D*). After a 10-min incubation in calcium-free buffer containing 0.1 mM EGTA, strong STIM2 puncta were evident in both shTRPC2 and shC cells. However, in mCherry-STIM1-expressing cells, we did not see any difference in the puncta formed in either shC or shTRPC2 cells even after a 10-min incubation in 0.1 mM EGTA buffer (Fig. 7, *E–H*). To ensure that the mCherry-STIM1 protein was functional, we

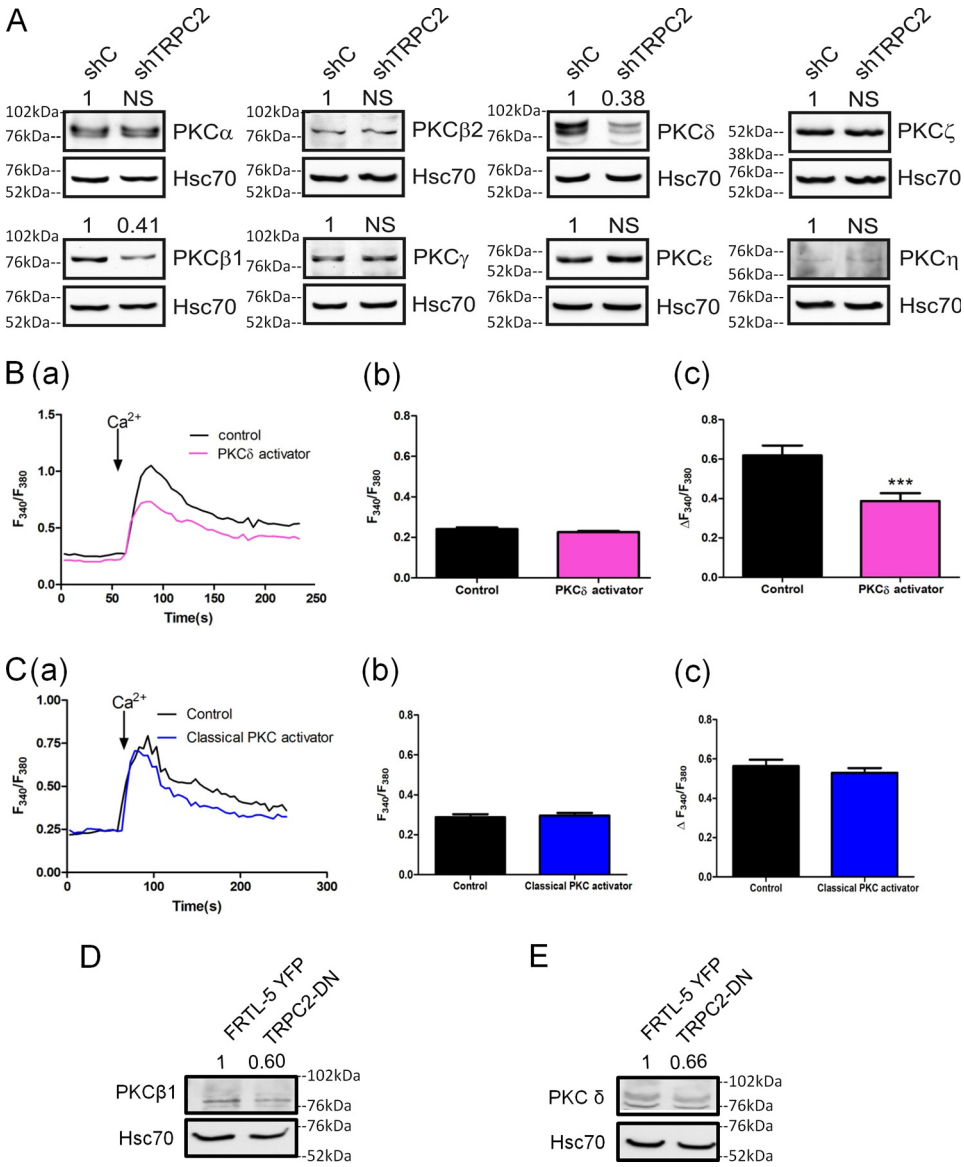

FIGURE 6. **PKCδ regulates basal calcium entry.** *A*, expression of different PKC isoforms in shC and shTRPC2 cells. Please note the decreased expression of PKCβ1 (shC, 1.0 ± 0.01; shTRPC2, 0.4 ± 0.08; $n = 4$; $p < 0.001$) and PKCδ (shC, 1.0 ± 0.04; shTRPC2, 0.4 ± 0.01; $n = 4$; $p < 0.001$) in shTRPC2 cells. Representative blots of at least three separate experiments are shown. The *number* above the blot indicates the relative amount of protein. *NS* denotes no significant change. *B*, *panel a*, representative traces of readdition of calcium (final concentration, 1 mM) to wild-type FRTL-5 cells pretreated with 5 μM PKCδ activator peptide for 2 h. *Panel b*, bar diagram showing the basal Fura-2 ratio before adding 1 mM Ca^{2+}. *Panel c*, bar diagram showing the increase in $[Ca^{2+}]_i$ after adding 1 mM Ca^{2+}. Each *bar* gives the mean ± S.E. (*error bar*) of at least 42 cells in each group (***, $p < 0.001$). *C*, *panel a*, representative traces of addition of calcium to wild-type FRTL-5 cells pretreated with a 5 μM concentration of a peptide activator of classical PKC isoforms for 2 h. *Panel b*, bar diagram showing the basal Fura-2 ratio before adding 1 mM Ca^{2+}. *Panel c*, bar diagram showing the increase in $[Ca^{2+}]_i$ after adding 1 mM Ca^{2+}. Each *bar* gives the mean ± S.E. (*error bar*) of at least 50 cells in each group. All the data shown were calculated from the changes in $[Ca^{2+}]_i$ from all cells measured, *i.e.* both responding and non-responding cells. *D* and *E*, expression of PKCβ1 (YFP, 1.0 ± 0.12; TRPC2-DN, 0.6 ± 0.04; $n = 4$; $p < 0.05$) and PKCδ (YFP, 1.0 ± 0.08; TRPC2-DN, 0.7 ± 0.03; $n = 4$; $p < 0.05$) in FRTL-5-YFP cells and TRPC2-DN cells. The *number* above the blot indicates the relative amount of protein.

treated the cells with Tg (1 μM for 10 min), and in these experiments, puncta were formed in both shC and shTRPC2 cells (supplemental Fig. 2, *A* and *B*). Additional images showing the STIM2-YFP expression in shC and shTRPC2 cells after 10-min incubation in 0.1 mM EGTA is also shown (supplemental Fig. 3, *A* and *B*).

Knockdown of PKCδ Enhanced Basal Calcium Entry, STIM2 Translocation to the Plasma Membrane, and Decreased SERCA Activity—To confirm a role for PKCδ or PKCβI in regulating the basal calcium entry, we down-regulated these PKC isoforms with siRNA in wild-type FRTL-5 cells (Fig. 8*A*). When either PKCβI (siPKCβ1) or PKCδ (siPKCδ) was down-regulated and calcium was readded to these cells in calcium-free buffer, the increase in $[Ca^{2+}]_i$ was enhanced compared with control (siC) cells (Fig. 8*B*). In unstimulated cells overexpressing YFP-tagged STIM2, an enhanced punctum formation was observed in siPKCδ, but not in siPKCβ, cells compared with siC cells (Fig. 8, *C* and *D*). Furthermore, the SERCA activity was attenuated in siPKCδ cells when compared with siC cells, whereas siRNA knockdown of PKCβ1 did not reduce the SERCA activity (Fig. 8*E*). Taken together, the results suggest that TRPC2 is of importance not only in regulating ago-

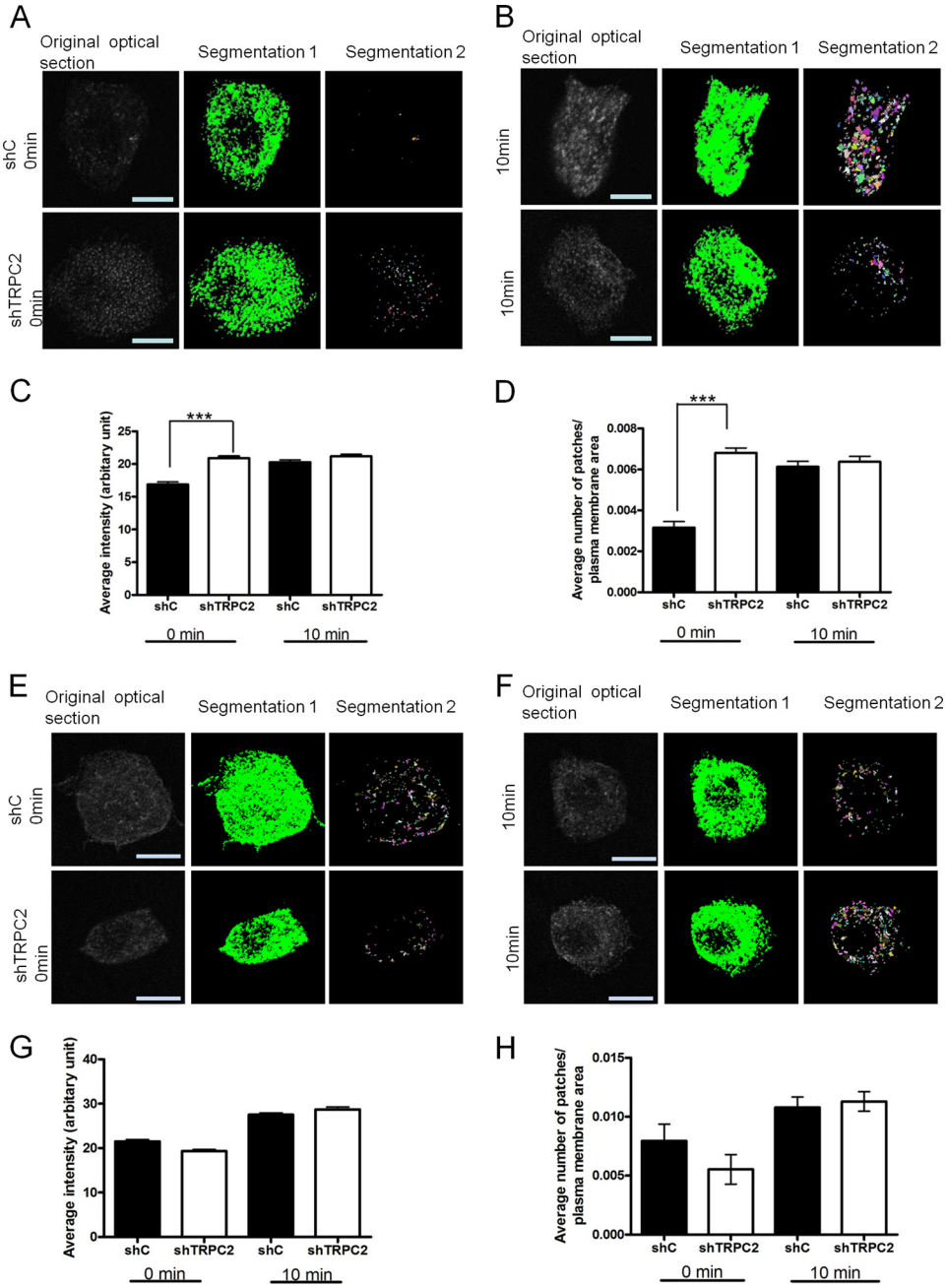

FIGURE 7. **TRPC2 knockdown enhances STIM2 punctum formation.** *A*, sample images showing confocal images of an shC and an shTRPC2 cell overexpressing YFP-STIM2 in a calcium-containing buffer prior to any treatment. *B*, as in *A*, but the cells were treated with 0.1 mM EGTA for 10 min. To improve the visualization, the original confocal sections were processed with a linear intensity transfer function (the same for every image). No color look-up table was utilized. The result of the segmentation used for intensity calculations is shown in *green*, and the result of the segmentation used for patch number calculations is shown with a different arbitrary color assigned for each patch. *Scale bar*, 10 μm. *C*, bar diagram showing the statistical analysis using the BioImageXD software of the average intensity of patches of YFP-STIM2 in shC and shTRPC2 cells. *D*, bar diagram showing the average number of patches of YFP-STIM2 in shC and shTRPC2 cells. *E*, sample images showing confocal images of an shC and an shTRPC2 cell overexpressing mCherry-STIM1 in a calcium-containing buffer prior to any treatment. *F*, as in *E*, but the cells were treated with 0.1 mM EGTA for 10 min. *G*, bar diagram showing the statistical analysis using the BioImageXD software of the average intensity of patches of mCherry-STIM1 in shC and shTRPC2 cells. *H*, bar diagram showing the average number of patches of mCherry-STIM1 in shC and shTRPC2 cells. Each *bar* gives the mean ± S.E. (*error bar*) of at least 15 images (***, $p < 0.001$).

nist-evoked calcium entry in FRTL-5 cells but also in regulating, possibly through PKCδ, SERCA activity and calcium content in the ER and as a result of this STIM2 translocation into membrane puncta and basal calcium entry.

Knockdown of STIM1 and STIM2 Attenuated Basal Calcium Entry in shTRPC2 Cells—STIM and Orai1 are the key regulators of SOCE (38, 39). Hence, we measured the expression of STIM1, STIM2, and Orai1 in shC and shTRPC2 cells. We did not find any significant differences in the expression of these proteins between the cells (Fig. 9, *A–C*). To study the role of STIM proteins in basal calcium entry, the expression of STIM1 and STIM2 was knocked down using siRNA (Fig. 9, *D* and *E*). siRNA knockdown of either STIM1 or STIM2 resulted in a significant decrease in basal calcium entry in shTRPC2 cells but not in shC cells (Fig. 9, *F* and *G*). To study the role of Orai1 in basal calcium entry, we used two

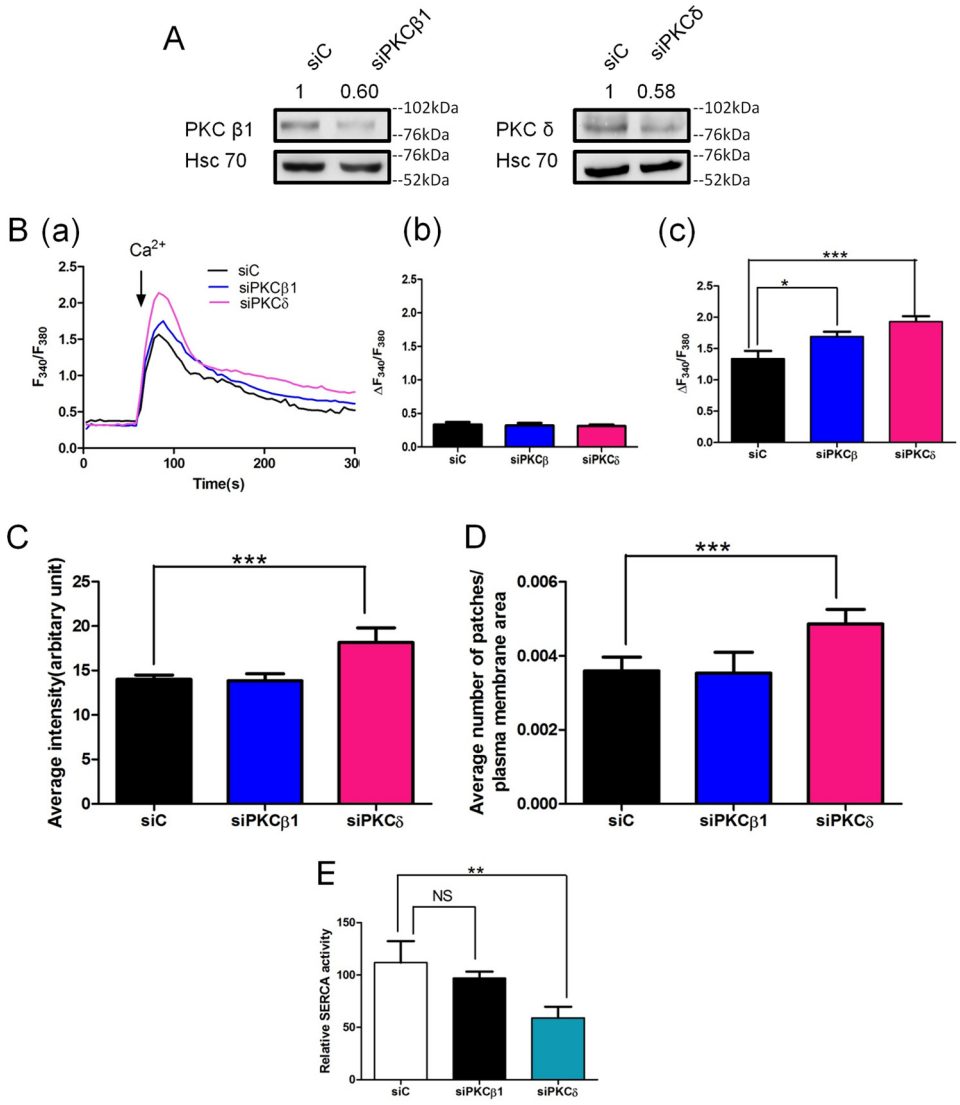

FIGURE 8. **Effects of knockdown of PKCδ on basal calcium entry, STIM2 translocation, and SERCA activity in wild-type FRTL-5 cells.** *A*, Western blot analysis of expression of PKCβ1 (siC, 1.0 ± 0.09; siPKCβ1, 0.6 ± 0.01; $n = 3$; $p < 0.05$) and PKCδ (siC, 1.0 ± 0.17; siPKCδ, 0.6 ± 0.08; $n = 4$; $p < 0.05$) in siRNA knockdown cells. The *number* above the blot indicates the relative amount of protein. *B*, *panel a*, representative traces of addition of 1 mM calcium to siC, siPKCβ1, and siPKCδ cells in a calcium-free buffer. *Panel b*, bar diagram showing the basal Fura-2 ratio before adding 1 mM Ca^{2+}. *Panel c*, bar diagram showing the increase in $[Ca^{2+}]_i$ after adding 1 mM Ca^{2+}. Each *bar* gives the mean ± S.E. (*error bar*) of at least 39 cells in each group. All the data shown were calculated from the changes in $[Ca^{2+}]_i$ from all cells measured, *i.e.* both responding and non-responding cells. *C*, bar diagram showing the statistic analysis using the BioImageXD software of the average intensity of patches of GFP-STIM2 in siC, siPKCβ1, and siPKCδ cells. *D*, bar diagram showing the average number of patches of GFP-STIM2 in siC, siPKCβ, and siPKCδ cells. Each *bar* gives the mean ± S.E. (*error bar*) of at least 15 images. *E*, SERCA activity of siC, siPKCβ1, and siPKCδ cells. Each *bar* gives the mean ± S.E. (*error bar*) of four experiments (*, $p < 0.05$; **, $p < 0.01$; ***, $p < 0.001$; *NS* denotes no significance).

mutants, a non-functional Orai1 R91W mutant (36) and an Orai1 S27A/S30A mutant (36) in which the PKC binding sites are mutated. Expression of either mutant resulted in decreased calcium entry in shTRPC2 cells (Fig. 9*H*). Thus, our results suggest that the increase in basal calcium entry in shTRPC2 cells is due to enhanced Orai1-STIM interactions.

DISCUSSION

In the present report we show, for the first time, that TRPC2 is a major regulator of calcium signaling in rat thyroid FRTL-5 cells. We show that the ATP-evoked calcium entry is mediated by TRPC2 at least in part. Furthermore, TRPC2 participates in regulating basal calcium entry in the cells probably by regulating the calcium content in the ER. We also show that the functional TRPC2 channel in FRTL-5 cells is a short TRPC2 splice variant. Our observations suggest that TRPC2 plays a more important role in regulating physiological events than previously believed.

Sequence databases contain several predicted sequences for rat TRPC2 splice variants, but to our knowledge, there are no published data on the function of the different TRPC2 variant proteins. We found that FRTL-5 cells express the short TRPC2 variants named F1MAE4 and Novel, and according to our results, F1MAE4 is a functional calcium channel whose knockdown has clear effects on calcium signaling. We did not address the function of the Novel variant in this study. It may work similarly to the mouse TRPC2 variant smTRPC2, which has been shown to modulate activity of other mouse TRPC2 vari-

ants (29). Like smTRPC2, Novel also represents a short N-terminal sequence of the predicted full-length TRPC2 and due to minimal transmembrane structure is perhaps unlikely to form a functional channel.

The regulation of TRPCs may occur via two major pathways (40–42). One pathway is activated by depletion of calcium stores in the endoplasmic reticulum as a result of receptor-evoked activation of phospholipase C, the production of DAG and IP_3, and the IP_3-evoked release of calcium from ER calcium stores. This results in translocation of STIM1 to puncta in the plasma membrane, complex formation with the Orai1 protein, and calcium entry (43). In some reports, TRPCs, in particular

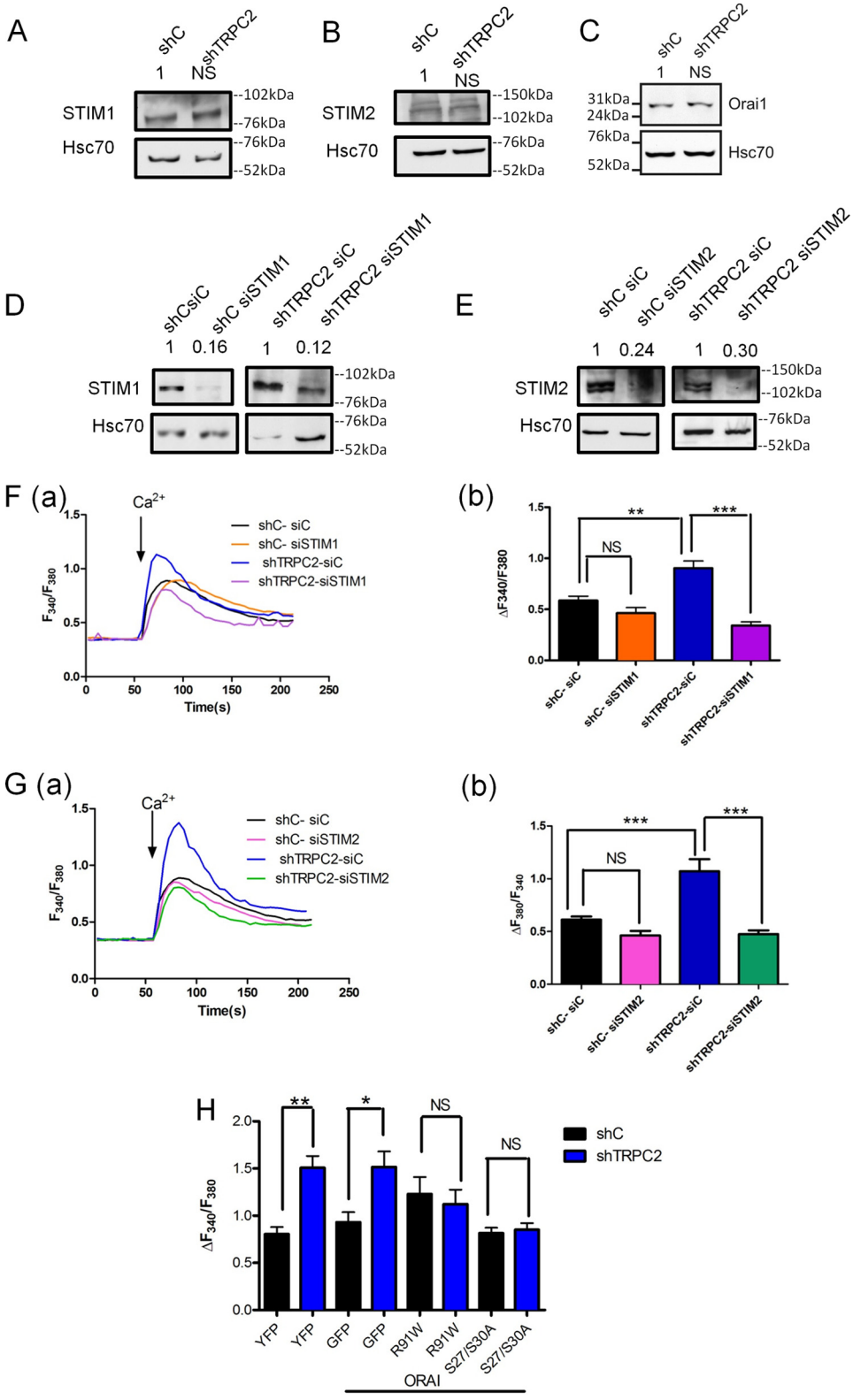

TRPC1 and -3, are part of this complex (40, 44, 45). The coupling of the adaptor protein Homer1 and IP_3 receptors with TRPCs may also participate in this regulation (46). Other studies have not observed an involvement of TRPCs (47). The other pathway is the result of receptor-mediated activation of TRPCs mediated by DAG (48). For TRPC2, this has been shown in neurons from the vomeronasal organ where a DAG-induced inward current was severely reduced in TRPC2 knock-out neurons (19). In sperm, which endogenously express TRPC2, an antibody against TRPC2 decreased both thapsigargin- and zona pellucida 3-induced calcium entry (18). Furthermore, inward currents were increased in HEK-293 cells transiently expressing TRPC2 after stimulation of purinergic receptors with ATP (18). Thus, TRPC2 can mediate both receptor-operated calcium entry and SOCE, and the mode of activation of the TRPC2 channel seems to be cell-specific, requiring different partners for signaling to proceed in different cells (21, 49–51). In our cells, the activation of TRPC2 seems to be exclusively receptor-mediated as the ATP-evoked calcium entry was attenuated in shTRPC2 cells, whereas the Tg-evoked SOCE was of the same magnitude in shC cells and shTRPC2 cells. In line with this, calcium entry was enhanced by the DAG analog OAG.

TRPC2 can bind to the IP_3 receptor either directly (19, 52–54) or through Homer1 (46, 55). In mouse erythroblasts, TRPC2, phospholipase C, and IP_3 receptors form a functional complex that regulates erythropoietin-evoked calcium release from the ER (21). In our cells, TRPC2 is apparently not involved in the receptor-evoked release of calcium from the ER as we did not observe any differences in the ATP-evoked calcium peak amplitude increase in calcium between shC and shTRPC2 cells when stimulated with ATP in a calcium-free buffer. However, a careful analysis showed that in calcium-free buffer the area under the curve of both the ATP-evoked and Tg-evoked calcium release was slightly, but significantly, smaller in shTRPC2 cells compared with shC cells. Readdition of calcium to cells in a calcium-free buffer resulted in an enhanced increase in cytosolic calcium in shTRPC2 cells compared with shC cells. This suggests that TRPC2 may participate in regulating ER calcium content. This is in line with the observed constitutive activity of TRPC2 in our cells (22).

Recent investigations have suggested that ER calcium sensor STIM2 is the master regulator of basal calcium entry, whereas STIM1 is of importance in SOCE. In a recent publication, Brandman *et al.* (56) showed that a small decrease in the calcium content of the ER resulted in a substantial translocation of STIM2 to puncta. In these experiments, no effect was seen on the translocation of STIM1. We observed a significant increase in STIM2 puncta in shTRPC2 cells and suggest that this is due to the decreased calcium content in the ER. We did not detect any significant difference in STIM1 localization between shTRPC2 cells and control cells. However, knockdown of either STIM1 or STIM2 with siRNA potently attenuated calcium entry in shTRPC2 cells but not in shC cells. The results suggest that STIM1 may also participate in regulating calcium entry (and store refilling) in shTRPC2 cells. ERK1/2 phosphorylation is dramatically increased in shTRPC2 cells (22). As STIM1 also can be found in the plasma membrane (57, 58) and as ERK1/2 phosphorylation of STIM1 is necessary for calcium entry (59), the enhanced ERK1/2 phosphorylation may explain our results. Presently no information regarding ERK1/2 and phosphorylation of STIM2 is available, but considering the very close homology between STIM1 and STIM2, we cannot exclude that ERK1/2 also affects STIM2, enhancing calcium uptake. Interestingly, PKC seems to have a crucial role in the translocation of STIM2 as knockdown of PKCδ resulted in an enhanced translocation of STIM2 into puncta.

PKC is a regulator of calcium entry in several cell types, including FRTL-5 cells (17). The mechanism is still unclear, but recent studies have shown that at least PKCβI phosphorylates Orai1, attenuating SOCE (36). In shTRPC2 cells, the expression of PKCβI and PKCδ was decreased. We do not know by what mechanism TRPC2 knockdown may decrease the expression of PKCβ1 and PKCδ, but by knockdown of PKCβ1 and PKCδ in native FRTL-5 cells, basal calcium entry was enhanced. As expected, when the cells were transfected with a non-conducting Orai1 mutant, the difference in calcium entry was abolished between shTRPC2 cells and shC cells. Interestingly, a similar result was obtained when the cells were transfected with an Orai1 mutant in which the PKC phosphorylation sites were mutated. Presently, we do not have an explanation for this surprising finding as the mutant significantly increased SOCE in a recent report (36).

However, the above results do not fully explain why the ER calcium load was smaller in shTRPC2 cells. In addition to regulating Orai1 and STIM phosphorylation (at least indirectly), PKC may also regulate SERCA function. Indeed, the SERCA activity in shTRPC2 cells was clearly decreased. Furthermore, expression of a truncated TRPC2 or down-regulation of PKCδ with siRNA also attenuated SERCA activity. Although the mechanism by which PKCδ may regulate SERCA function is unclear in our cells, the decreased SERCA activity probably explains the smaller ER calcium content in shTRPC2 cells. This in turn induced STIM2 punctum formation and increased basal calcium entry.

FIGURE 9. **siRNA knockdown of STIM1 and STIM2 and transfection with mutant Orai1 decrease basal calcium influx in shTRPC2 cells.** *A*, *B*, and *C*, Western blot analysis shows no significant difference in the expression of STIM1 (shC, 1.0 ± 0.08; shTRPC2, 1.3 ± 0.01; $n = 3$), STIM2 (shC, 1.0 ± 0.19; shTRPC2, 1.1 ± 0.24; $n = 3$), and Orai1 (shC, 1.0 ± 0.07; shTRPC2, 0.9 ± 0.24; $n = 4$), respectively, in shC and shTRPC2 cells. *NS* denotes no significance. *D*, Western blots showing knockdown of STIM1 using siRNA (shC-siC, 1.0 ± 0.29; shC-STIM1, 0.2 ± 0.03; $n = 3$; $p < 0.05$; shTRPC2-siC, 1.0 ± 0.20; shTRPC2-siSTIM1, 0.1 ± 0.03; $n = 3$; $p < 0.05$). *E*, Western blots showing knockdown of STIM2 using siRNA (shC-siC, 1.0 ± 0.37; shC-siSTIM2; 0.2 ± 0.03; $n = 5$; $p < 0.05$; shTRPC2-siC, 1.0 ± 0.16; shTRPC2-siSTIM2, 0.3 ± 0.09; $n = 5$; $p < 0.001$). The *number* above the blot indicates the relative amount of protein. *F*, *panel a*, representative traces of addition of 1 mM calcium to shC-siC, shC-STIM1, shTRPC2-siC, and shTRPC2-siSTIM1 cells. *Panel b*, bar diagram showing the increase in $[Ca^{2+}]_i$ after adding 1 mM Ca^{2+}. Each *bar* gives the mean ± S.E. (*error bar*) of at least 40 cells in each group. *G*, *panel a*, representative traces of addition of 1 mM calcium to shC-siC, shC-STIM2, shTRPC2-siC, and shTRPC2-siSTIM2 cells. *Panel b*, bar diagram showing the increase in $[Ca^{2+}]_i$ after adding 1 mM Ca^{2+}. Each *bar* gives the mean ± S.E. (*error bar*) of at least 40 cells in each group. *H*, transfection with the Orai1 R91W or the Orai1 S27A/S30A mutant abolished the difference in basal calcium entry between shC and shTRPC2 cells. Calcium (final concentration, 1 mM) was readded to cells in a calcium-free buffer, and the increase in $[Ca^{2+}]_i$ was measured. The *bars* give the mean ± S.E. (*error bars*) of at least 30 cells (*NS*, not significant; *, $p < 0.05$; **, $p < 0.01$; ***, $p < 0.001$). All the data shown were calculated from the changes in $[Ca^{2+}]_i$ from all cells measured, *i.e.* both responding and non-responding cells.

In conclusion, we have shown that rat thyroid FRTL-5 cells express only the TRPC2 channel of the TRPC family of ion channels. In these cells, TRPC2 functions as a receptor-operated calcium channel. In addition, our data suggest that TRPC2 participates in regulating basal calcium entry. We propose that in addition to its receptor-operated mode of action TRPC2 can participate in the regulation of ER calcium content by modulating PKC expression and SERCA activity. Our results suggest that TRPC2 is a master regulator of cellular calcium homeostasis in rat thyroid cells and thus reveal a novel function for the channel.

Acknowledgments—We thank Dr. Richard S Lewis (Stanford University), Dr. Tobias Meyer (Stanford University), Dr. Catherine Dulac (Harvard University), Dr. Anjana Rao (Harvard University), Dr. Genevieve Bart (University of Eastern Finland), and Dr. Stefan Feske (New York University) for sharing plasmids.

REFERENCES

1. Berridge, M. J., Bootman, M. D., and Roderick, H. L. (2003) Calcium signalling: dynamics, homeostasis and remodelling. *Nat. Rev. Mol. Cell Biol.* **4,** 517–529
2. Weiss, S. J., Philp, N. J., and Grollman, E. F. (1984) Iodide transport in a continuous line of cultured cells from rat thyroid. *Endocrinology* **114,** 1090–1098
3. Corda, D., Marcocci, C., Kohn, L. D., Axelrod, J., and Luini, A. (1985) Association of the changes in cytosolic Ca^{2+} and iodide efflux induced by thyrotropin and by the stimulation of α_1-adrenergic receptors in cultured rat thyroid cells. *J. Biol. Chem.* **260,** 9230–9236
4. Berman, M. I., Thomas, C. G., Jr., and Nayfeh, S. N. (1987) Stimulation of inositol phosphate formation in FRTL-5 rat thyroid cells by catecholamines and its relationship to changes in $^{45}Ca^{2+}$ efflux and cyclic AMP accumulation. *Mol. Cell. Endocrinol.* **54,** 151–163
5. Törnquist, K., Ekokoski, E., and Dugué, B. (1996) Purinergic agonist ATP is a comitogen in thyroid FRTL-5 cells. *J. Cell Physiol.* **166,** 241–248
6. Ekokoski, E., Webb, T. E., Simon, J., and Törnquist, K. (2001) Mechanisms of P2 receptor-evoked DNA synthesis in thyroid FRTL-5 cells. *J. Cell. Physiol.* **187,** 166–175
7. Okajima, F., Tokumitsu, Y., Kondo, Y., and Ui, M. (1987) P_2-purinergic receptors are coupled to two signal transduction systems leading to inhibition of cAMP generation and to production of inositol trisphosphate in rat hepatocytes. *J. Biol. Chem.* **262,** 13483–13490
8. Saji, M., Ikuyama, S., Akamizu, T., and Kohn, L. D. (1991) Increases in cytosolic Ca^{++} down regulate thyrotropin receptor gene expression by a mechanism different from the cAMP signal. *Biochem. Biophys. Res. Commun.* **176,** 94–101
9. Di Jeso, B., Pereira, R., Consiglio, E., Formisano, S., Satrustegui, J., and Sandoval, I. V. (1998) Demonstration of a Ca^{2+} requirement for thyroglobulin dimerization and export to the Golgi complex. *Eur. J. Biochem.* **252,** 583–590
10. Rivas, M., Mellström, B., Naranjo, J. R., and Santisteban, P. (2004) Transcriptional repressor DREAM interacts with thyroid transcription factor-1 and regulates thyroglobulin gene expression. *J. Biol. Chem.* **279,** 33114–33122
11. Raspé, E., Laurent, E., Andry, G., and Dumont, J. E. (1991) ATP, bradykinin, TRH and TSH activate the Ca^{2+}-phosphatidylinositol cascade of human thyrocytes in primary culture. *Mol. Cell. Endocrinol.* **81,** 175–183
12. Sho, K. M., Okajima, F., Abdul Majid, M., and Kondo, Y. (1991) Reciprocal modulation of thyrotropin actions by P_1-purinergic agonists in FRTL-5 thyroid cells. Inhibition of cAMP pathway and stimulation of phospholipase C-Ca^{2+} pathway. *J. Biol. Chem.* **266,** 12180–12184
13. Törnquist, K. (1992) Evidence for receptor-mediated calcium entry and refilling of intracellular calcium stores in FRTL-5 rat thyroid cells. *J. Cell Physiol.* **150,** 90–98
14. Törnquist, K., Saarinen, P., Vainio, M., and Ahlström, M. (1997) Sphingosine 1-phosphate mobilizes sequestered calcium, activates calcium entry, and stimulates deoxyribonucleic acid synthesis in thyroid FRTL-5 cells. *Endocrinology* **138,** 4049–4057
15. Okajima, F., Tomura, H., Sho, K., Kimura, T., Sato, K., Im, D. S., Akbar, M., and Kondo, Y. (1997) Sphingosine 1-phosphate stimulates hydrogen peroxide generation through activation of phospholipase C-Ca^{2+} system in FRTL-5 thyroid cells: possible involvement of guanosine triphosphate-binding proteins in the lipid signaling. *Endocrinology* **138,** 220–229
16. Grasberger, H., Van Sande, J., Hag-Dahood Mahameed, A., Tenenbaum-Rakover, Y., and Refetoff, S. (2007) A familial thyrotropin (TSH) receptor mutation provides *in vivo* evidence that the inositol phosphates/Ca^{2+} cascade mediates TSH action on thyroid hormone synthesis. *J. Clin. Endocrinol. Metab.* **92,** 2816–2820
17. Törnquist, K. (1993) Modulatory effect of protein kinase C on thapsigargin-induced calcium entry in thyroid FRTL-5 cells. *Biochem. J.* **290,** 443–447
18. Jungnickel, M. K., Marrero, H., Birnbaumer, L., Lémos, J. R., and Florman, H. M. (2001) Trp2 regulates entry of Ca^{2+} into mouse sperm triggered by egg ZP3. *Nat. Cell Biol.* **3,** 499–502
19. Lucas, P., Ukhanov, K., Leinders-Zufall, T., and Zufall, F. (2003) A diacylglycerol-gated cation channel in vomeronasal neuron dendrites is impaired in TRPC2 mutant mice: mechanism of pheromone transduction. *Neuron* **40,** 551–561
20. Liman, E. R.(2003) Regulation by voltage and adenine nucleotides of a Ca^{2+}-activated cation channel from hamster vomeronasal sensory neurons. *J. Physiol.* **548,** 777–787
21. Chu, X., Cheung, J. Y., Barber, D. L., Birnbaumer, L., Rothblum, L. I., Conrad, K., Abrasonis, V., Chan, Y.-M., Stahl, R., Carey, D. J., and Miller, B. A. (2002) Erythropoietin modulates calcium influx through TRPC2. *J. Biol. Chem.* **277,** 34375–34382
22. Löf, C. Sukumaran, P., Viitanen, T., Vainio, M., Kemppainen, K., Pulli, I., Näsman, J., Kukkonen, J., and Törnquist, K. (2012) Communication between the calcium and cAMP pathways regulate the expression of the thyroid-stimulating hormone receptor: TRPC2 in the center of action. *Mol. Endocrinol.*, in press
23. Larsson, K. P., Peltonen, H. M., Bart, G., Louhivuori, L. M., Penttonen, A., Antikainen, M., Kukkonen, J. P., and Akerman, K. E. (2005) Orexin-A-induced Ca^{2+} entry: evidence for involvement of TRPC channels and protein kinase C regulation. *J. Biol. Chem.* **280,** 1771–1781
24. Chen, L., Hahn, H., Wu, G., Chen, C. H., Liron, T., Schechtman, D., Cavallaro, G., Banci, L., Guo, Y., Bolli, R., Dorn, G. W., 2nd, and Mochly-Rosen, D. (2001) Opposing cardioprotective actions and parallel hypertrophic effects of δ PKC and ϵ PKC. *Proc. Natl. Acad. Sci. U.S.A.* **98,** 11114–11119
25. Churchill, E. N., Qvit, N., and Mochly-Rosen, D. (2009) Rationally designed peptide regulators of protein kinase C. *Trends Endocrinol. Metab.* **20,** 25–33
26. Löf, C., Blom, T., and Törnquist, K. (2008) Overexpression of TRPC3 reduces the content of intracellular calcium stores in HEK-293 cells. *J. Cell. Physiol.* **216,** 245–252
27. Hamill, O. P., Marty, A., Neher, E., Sakmann, B., and Sigworth, F. J. (1981) Improved patch-clamp techniques for high-resolution current recording from cells and cell-free membrane patches. *Pflugers Arch.* **391,** 85–100
28. Barry, P. H. (1994) JPCalc, a software package for calculating liquid junction potential corrections in patch-clamp, intracellular, epithelial and bilayer measurements and for correcting junction potential measurements. *J. Neurosci. Methods* **51,** 107–116
29. Chu, X., Tong, Q., Wozney, J., Zhang, W., Cheung, J. Y., Conrad, K., Mazack, V., Stahl, R., Barber, D. L., and Miller, B. A. (2005) Identification of an N-terminal TRPC2 splice variant which inhibits calcium influx. *Cell Calcium* **37,** 173–182
30. Wang, L., Wang, L., Song, R., Shen, Y., Sun, Y., Gu, Y., Shu, Y., and Xu, Q. (2011) Targeting sarcoplasmic/endoplasmic reticulum Ca^{2+}-ATPase 2 by curcumin induces ER stress-associated apoptosis for treating human liposarcoma. *Mol. Cancer Ther.* **10,** 461–471
31. Kankaanpää, P., Paavolainen, L., Tiitta, S., Karjalainen, M., Päivärinne, J., Nieminen, J., Marjomäki, V., Heino, J., and White, D. J. (2012) BioIm-

ageXD: an open, general-purpose and high-throughput image-processing platform. *Nat. Methods* **9,** 683–689
32. Alvarez, J., Coulombe, A., Cazorla, O., Ugur, M., Rauzier, J.-M., Magyar, J., Mathieu, E.-L., Boulay, G., Souto, R., Bideaux, P., Salazar, G., Rassendren, F., Lacampagne, A., Fauconnier, J., and Vassort, G. (2008) ATP/UTP activate cation-permeable channels with TRPC3/7 properties in rat cardiomyocytes. *Am. J. Physiol. Heart Circ. Physiol.* **295,** H21–H28
33. McCollum, A. T., Jafarifar, F., Chan, R., and Guttmann, R. P. (2004) Oxidative stress inhibits ionomycin-mediated cell death in cortical neurons. *J. Neurosci. Res.* **76,** 104–109
34. Arruda, A. P., Nigro, M., Oliveira, G. M., and de Meis, L. (2007) Thermogenic activity of Ca^{2+}-ATPase from skeletal muscle heavy sarcoplasmic reticulum: the role of ryanodine Ca^{2+} channel. *Biochim. Biophys. Acta* **1768,** 1498–1505
35. Højmann Larsen, A., Frandsen, A., and Treiman, M. (2001) Upregulation of the SERCA-type Ca^{2+} pump activity in response to endoplasmic reticulum stress in PC12 cells. *BMC Biochem.* **2,** 4
36. Kawasaki, T., Ueyama, T., Lange, I., Feske, S., and Saito, N. (2010) Protein kinase C-induced phosphorylation of Orai1 regulates the intracellular Ca^{2+} level via the store-operated Ca^{2+} channel. *J. Biol. Chem.* **285,** 25720–25730
37. Sutton, K. A., Jungnickel, M. K., Wang, Y., Cullen, K., Lambert, S., and Florman, H. M. (2004) Enkurin is a novel calmodulin and TRPC channel binding protein in sperm. *Dev. Biol.* **274,** 426–435
38. Deng, X., Wang, Y., Zhou, Y., Soboloff, J., and Gill, D. L. (2009) STIM and Orai: dynamic intermembrane coupling to control cellular calcium signals. *J. Biol. Chem.* **284,** 22501–22505
39. DeHaven, W. I., Jones, B. F., Petranka, J. G., Smyth, J. T., Tomita, T., Bird, G. S., and Putney, J. W., Jr. (2009) TRPC channels function independently of STIM1 and Orai1. *J. Physiol.* **587,** 2275–2298
40. Liu, X., Wang, W., Singh, B. B., Lockwich, T., Jadlowiec, J., O'Connell, B., Wellner, R., Zhu, M. X., and Ambudkar, I. S. (2000) Trp1, a candidate protein for the store-operated Ca^{2+} influx mechanism in salivary gland cells. *J. Biol. Chem.* **275,** 3403–3411
41. Boulay, G. (2002) Ca^{2+}-calmodulin regulates receptor-operated Ca^{2+} entry activity of TRPC6 in HEK-293 cells. *Cell Calcium* **32,** 201–207
42. Worley, P. F., Zeng, W., Huang, G. N., Yuan, J. P., Kim, J. Y., Lee, M. G., and Muallem, S. (2007) TRPC channels as STIM1-regulated store-operated channels. *Cell Calcium* **42,** 205–211
43. Liou, J., Kim, M. L., Heo, W. D., Jones, J. T., Myers, J. W., Ferrell, J. E., Jr., and Meyer, T. (2005) STIM is a Ca^{2+} sensor essential for Ca^{2+}-store-depletion-triggered Ca^{2+} influx. *Curr. Biol.* **15,** 1235–1241
44. Huang, G. N., Zeng, W., Kim, J. Y., Yuan, J. P., Han, L., Muallem, S., and Worley, P. F. (2006) STIM1 carboxyl-terminus activates native SOC, I_{crac} and TRPC1 channels. *Nat. Cell Biol.* **8,** 1003–1010
45. Zagranichnaya, T. K., Wu, X., and Villereal, M. L. (2005) Endogenous TRPC1, TRPC3, and TRPC7 proteins combine to form native store-operated channels in HEK-293 cells. *J. Biol. Chem.* **280,** 29559–29569
46. Stiber, J. A., Zhang, Z.-S., Burch, J., Eu, J. P., Zhang, S., Truskey, G. A., Seth, M., Yamaguchi, N., Meissner, G., Shah, R., Worley, P. F., Williams, R. S., and Rosenberg, P. B. (2008) Mice lacking Homer 1 exhibit a skeletal myopathy characterized by abnormal transient receptor potential channel activity. *Mol. Cell. Biol.* **28,** 2637–2647
47. Salido, G. M., Sage, S. O., and Rosado, J. A. (2009) TRPC channels and store-operated Ca^{2+} entry. *Biochim. Biophys. Acta* **1793,** 223–230
48. Dietrich, A., Mederos y Schnitzler, M., Kalwa, H., Storch, U., and Gudermann, T. (2005) Functional characterization and physiological relevance of the TRPC3/6/7 subfamily of cation channels. *Naunyn Schmiedebergs Arch. Pharmacol.* **371,** 257–265
49. Villereal, M. L. (2006) Mechanism and functional significance of TRPC channel multimerization. *Semin. Cell Dev. Biol.* **17,** 618–629
50. Yildirim, E., and Birnbaumer, L. (2007) TRPC2: molecular biology and functional importance. *Handb. Exp. Pharmacol.* **179,** 53–75
51. Abramowitz, J., and Birnbaumer, L. (2009) Physiology and pathophysiology of canonical transient receptor potential channels. *FASEB J.* **23,** 297–328
52. Yuan, J. P., Kiselyov, K., Shin, D. M., Chen, J., Shcheynikov, N., Kang, S. H., Dehoff, M. H., Schwarz, M. K., Seeburg, P. H., Muallem, S., and Worley, P. F. (2003) Homer binds TRPC family channels and is required for gating of TRPC1 by IP3 receptors. *Cell* **114,** 777–789
53. Tong, Q., Chu, X., Cheung, J. Y., Conrad, K., Stahl, R., Barber, D. L., Mignery, G., and Miller, B. A. (2004) Erythropoietin-modulated calcium influx through TRPC2 is mediated by phospholipase Cγ and IP3R. *Am. J. Physiol. Cell Physiol.* **287,** C1667–C1678
54. Yildirim, E., Dietrich, A., and Birnbaumer, L. (2003) The mouse C-type transient receptor potential 2 (TRPC2) channel: alternative splicing and calmodulin binding to its N terminus. *Proc. Natl. Acad. Sci. U.S.A.* **100,** 2220–2225
55. Mast, T. G., Brann, J. H., and Fadool, D. A. (2010) The TRPC2 channel forms protein-protein interactions with Homer and RTP in the rat vomeronasal organ. *BMC Neurosci.* **11,** 61
56. Brandman, O., Liou, J., Park, W. S., and Meyer, T. (2007) STIM2 is a feedback regulator that stabilizes basal cytosolic and endoplasmic reticulum Ca^{2+} levels. *Cell* **131,** 1327–1339
57. Manji, S. S., Parker, N. J., Williams, R. T., van Stekelenburg, L., Pearson, R. B., Dziadek, M., and Smith, P. J. (2000) STIM1: a novel phosphoprotein located at the cell surface. *Biochim. Biophys. Acta* **1481,** 147–155
58. Spassova, M. A., Soboloff, J., He, L.-P., Xu, W., Dziadek, M. A., and Gill, D. L. (2006) STIM1 has a plasma membrane role in the activation of store-operated Ca^{2+} channels. *Proc. Natl. Acad. Sci. U.S.A.* **103,** 4040–4045
59. Pozo-Guisado, E., Campbell, D. G., Deak, M., Alvarez-Barrientos, A., Morrice, N. A., Alvarez, I. S., Alessi, D. R., and Martín-Romero, F. J. (2010) Phosphorylation of STIM1 at ERK1/2 target sites modulates store-operated calcium entry. *J. Cell Sci.* **123,** 3084–3093